Drug Design, Development and Therapy

Dovepress
Taylor & Francis Group

Open Access Full Text Article

ORIGINAL RESEARCH

Designing, Characterization, and Optimization of Nystatin Loaded Mucoadhesive Spanlastical Hard Candy Lozenges as a Treatment of Oral Candidiasis: An in-vivo Study on Rats

Raghda Rabe Hamed[1], Azza Ali Musafer Al-Khathami[2], Eyman M Eltayib[3,4], Reem Mohammed Ayed Al-Qarni[2], Rania A Hussien[5], Reem F Alshehri[6], Mona Alhamod[7,8], Bayan Alkhaldi[3,8]

[1]Department of Industrial Pharmacy, College of Pharmaceutical Sciences and Drug Manufacturing, Misr University for Science and Technology (MUST), 6th of October City, Giza, Egypt; [2]Department of Chemistry, College of Art and Science, Bisha University, Balqarn, Kingdom of Saudi Arabia; [3]Department of Pharmaceutics, Faculty of Pharmacy, Jouf University, Sakaka, Kingdom of Saudi Arabia; [4]Department of Pharmaceutics, Faculty of Pharmacy, AL Neelain University, Khartoum, Sudan; [5]Department of Chemistry, College of Science, Al Baha University, Al Baha, Kingdom of Saudi Arabia; [6]Department of Chemistry, College of Science, Taibah University, Medina, Kingdom of Saudi Arabia; [7]Department of Pharmaceutics, Faculty of Pharmacy, Northern Border University, Arar, Kingdom of Saudi Arabia; [8]School of Pharmacy, Queen's University Belfast, Belfast, UK

Correspondence: Raghda Rabe Hamed, Department of Industrial Pharmacy, College of Pharmaceutical Sciences and Drug Manufacturing, Misr University for Science and Technology (MUST), P.O. Box 77, 6th October City, Giza, Egypt, Tel +20 01151144222, Email Raghda.hamid@must.edu.eg

Introduction and Aim: Oral candidiasis is a common infectious disease affecting children and adults who usually receive oral antibiotics or chemotherapy. Optimizing Nystatin administration is challenging due to its poor solubility and systemically non-absorbable nature. In this work, Nystatin Spanlastical-hard candies were prepared for Oro-local application to improve Nystatin's local antifungal efficacy, contact time, and taste.

Methods: Eight Nystatin Spanlastics were prepared using the ethanol injection method via 2^3 factorial designs using Span, edge activator, and bath-sonication time at two levels. They were evaluated visually and examined for EE%, in-vitro release%, P-size, PDI, and Zeta-potential. The optimum formulae were compared to the marketed oral suspension Nystatin® by conducting an in-vitro antimicrobial study. The formula of the best antifungal activity was incorporated into four batches of hard candies by 2^2 factorial-design using heating and congealing method using corn-syrup and xanthan-gum in two levels of concentration along with other additives. After performing physiochemical evaluation, the optimum formula was subjected to FTIR analysis and an in-vivo study on rats to compare its activity with the selected market formula. The Design-Expert-13® and MS-Excel-2010® software were used to interpret all results statistically.

Results: The optimum Spanlastical formula was Sp3, which is a combination of Span 80 with SDC, and was sonicated for 3 minutes. The optimum lozenges were those of the SP3L1 batch containing the highest Corn syrup and Xanthan gum concentration levels. SP3L1 lozenges showed no interactions between their ingredients within the obtained FTIR spectra. They gave the animal subjects a higher in-vivo antifungal activity with a significant reduction in the colony formation units' count at $P \leq 0.05$ than the (Nystatin) marketed oral suspension. The rats also treated with SP3L1 showed very normal oral tissues by the end of the study period compared to those treated with the market oral formula (Nystatin).

Conclusion: This preclinical study merged nanotechnology with mucoadhesive lozenging to improve Nystatin's antifungal activity, oral residence, and ease of administration compared to the traditionally marketed oral suspension.

Keywords: Nystatin, candidiasis, spanlastical candy, mucoadhesive lozenges, in-vivo study

Introduction

Local drug delivery is a relatively painless technique that delivers therapeutic substances directly to a specific tissue, enhances their efficacy, and decreases their side effects.[1] Buccal drug delivery systems such as lozenges bring the compounds into direct contact with the mucosal oral cavity to treat local and systemic diseases. Medicated Lozenges are flavored and sweetened solid

Received: 5 November 2024
Accepted: 24 March 2025
Published: 28 April 2025

dosage forms that are designed to be sucked and held in the oral cavity to enhance the loaded drug's oral retention and so increase their bioavailability. The buccal mucosa is a highly vascularized tissue with a rich blood supply that helps them bypass gastric irritation and both gastric and hepatic first-pass metabolism.[2]

The oral dissolution time of lozenges is patient-dependent as the patient can control the dissolution rate and then absorption by controlling the lozenge-sucking speed until it completely dissolves; however, lozenges generally take maximally about 30 minutes to be completely dissolved. Lozenges have broad clinical potential as they can be used to deliver various active ingredients, such as cough suppressants, pain relievers, probiotics, vaccines, and antibiotics.[3,4]

Lozenges can be a practical and effective treatment choice for both children and the elderly, especially being colorful, tasty, attractive, and convenient. However, using the medicated lozenges for children and the elderly has many challenges, such as the medicinal aftertaste that can affect their compliance. Also, potential risks of overdose and choking can happen.[2]

Spanlastics are nano-vesicular drug delivery systems composed of vesicle-forming agents and edge activators. They are carriers known to have a highly elastic wall membrane and can deliver drugs non-invasively through the different membrane barriers. They are generally used for both local and systemic delivery of drugs such as proteins, peptides, and hormones.[5,6] Nystatin is a polyene antifungal drug with broad-spectrum fungicidal and fungistatic activity against several yeasts and fungi, notably Candida. It is not absorbed from the gastrointestinal tract when administered orally. Therefore, the topical preparations of Nystatin are the most common in the pharmaceutical industry.[7] The present preclinical study focused on developing an attractive flavored Spanlastical-hard candy of Nystatin for the local treatment of oral candidiasis, especially for the elderly and children who get oral candidiasis post-antibiotic or chemotherapy treatments. It provides ease of administration, enhanced taste, prolonged oral residence, and high antifungal efficacy.

Materials and Methods

Materials

Nystatin was kindly supplied as a gift by Epico Pharmaceutical Co., Cairo, Egypt. Span60, Span80, Tween 20, and Sodium deoxycholate were purchased from Sigma Chemical Co., USA. Sodium dihydrogen phosphate monobasic dihydrate and sodium hydrogen phosphate dibasic anhydrous were purchased from ADWIC, Cairo, Egypt. *C. albicans* of American Type Culture Collection (ATCC10231) was a gift from the microbiology department, faculty of pharmacy, Cairo University. Sabouraud dextrose agar was purchased from Difco™, USA. β-cyclodextrin, Mannitol, Acacia, Xanthan gum, Corn syrup, and microcrystalline cellulose were purchased from Al-Shark AL-Awsat Company, Cairo, Egypt. Orange Colour (Sunset yellow grade FCF E110) was purchased from Tradeasia International DMCC Inc., Dubai, UAE. Orange oil flavor was purchased from Komesz Flavours company, Shanghai, China. Ethanol and methanol of HPLC grade were purchased from Sigma-Aldrich Co., USA.

Methods

Nystatin Nano-Spanlastics

Formulation of Nystatin Nano-Spanlastics Using Different EAs

Nystatin Spanlastics were prepared using the ethanol injection technique reported by Kakkar and Kaur.[8] In brief, Eight Nystatin-loaded Spanlastics were prepared using a 2^3-factorial design, considering the Span grades, Edge activator type, and bath sonication time at two levels. Center points were added to confirm the non-significance of curvature of the selected models using the Design Expert—13® program,[9] as shown in Table 1.

In a parafilm-covered 100 mL beaker, ethanol was used to dissolve 10 mg of Nystatin (equivalent to 5000 IU potency per mg), and 450 mg of the selected Span type in a 70°C water bath until a clear solution was obtained. Ethanol was the organic solvent chosen as it can solubilize both the drug and the vesicle-forming agent (Span). It has a rabid evaporation time that can accelerate the overall process.[9–11] The ethanolic solution was injected dropwise using a syringe pump into an aqueous phase of the same temperature containing 50 mg of the selected EA at 1 mL/min rate.[12] The ratio of the ethanolic phase to the aqueous one was 1:4. The mixture was continuously stirred using the magnetic stirrer (LMS-1003, Kyonggi-Do, Korea) at 350 rpm, maintaining the same temperature until the formation of SPs aqueous dispersions. The prepared

Table 1 The Levels of the Independent Variables Used to Formulate Nystatin Loaded Nano-Spanlastics Utilizing (2^3) Full Factorial Design

Factors (Independent Variables)	**Levels**	
X1: Span Type	Span60	Span80
X2: Edge activator type	Tween 20	SDC
X3: Ultrasonication time	3 min	5 min
Responses (Dependent Variables)	**Desirability Constraint**	
Y1: EE%	Maximize	
Y2: In-vitro release %	Maximize	
Y3: VS (nm)	Minimize	
Y4: PDI	Minimize	
Y5: ZP (mV)	Maximize (as absolute value)	

Abbreviations: SDC, Sodium Deoxy Cholate; EE%, Entrapment Efficiency percent; VS, Vesicle Size; PDI, Poly Dispersity Index; ZP, Zeta Potential.

5000 IU/ mL Nystatin-loaded nano-Spanlastics were stirred at 1000 rpm at room temperature until the complete evaporation of any remaining ethanol. Then, water-bath ultrasonication at 25°C was applied for the selected time to reduce the vesicle size (Crest Ultrasonics Corp, Trenton, USA). The Spanlastical dispersions were stored at four °C until further investigations were performed.[13,14] The composition of the prepared Nystatin Spanlastics is shown in Table 2.

Evaluation of Nystatin Medicated Spanlastical Dispersions

Visual Inspection. The features and other properties of the freshly prepared Spanlastical dispersions, including color, turbidity, odor, and dispersibility, were investigated. All formulae were examined visually for their degree of turbidity above black-and-white backgrounds and then rated as clear (+), slightly turbid (++), or highly turbid (+++). After shaking for one minute, all preparations were evaluated as dispersible or non-dispersible.

Table 2 The Composition of the Nystatin Nano-Spanlastics According to the Selected 2^3 Full Factorial Design

Formula	**Span Grade (mg) X1**		**EA Type (mg) X2**		**Ultrasonication Time (min) X3**
	Span60	**Span80**	**Tween 20**	**SDC**	
SP1	450	–	50	–	3
SP2	450	–	50	–	5
SP3	–	450	–	50	3
SP4	–	450	–	50	5
SP5	450	–	–	50	3
SP6	450	–	–	50	5
SP7	–	450	50	–	3
SP8	–	450	50	–	5

Abbreviations: EA, Edge activator; SDC, Sodium Deoxy Cholate.

Determination of Entrapment Efficiency (EE%). One mL of each formula was first dissolved in methanol. The absorbance was measured at 279nm (λ_{max} of Nystatin in methanol) to calculate the actual total drug content in each formula (Free + entrapped) using a UV spectrophotometer (Shimadzu UV 1650, Japan). Another one mL of each preparation was centrifuged for 50 min at 14,000 rpm at four °C using the ultra-cooling centrifuge (Beckman, Fullerton, Canada) to separate the precipitated Spanlastical vesicles. The separated precipitates were then washed with a phosphate buffer of pH 6.8, isolated again carefully using the same conditions, and then disrupted by sonication with methanol to estimate the Nystatin amount entrapped inside the formed vesicles spectrophotometrically at the same λ_{max}. The entrapment efficiency was then calculated according to the provided equation, and each result was the mean of three determinations ±SD.[15] The results were interpreted using the (Design Expert-13) program.

$$EE\% = \left[\frac{Amount\ of\ NYS\ entrapped\ (\mu g)}{Total\ amount\ of\ NYS\ (\mu g)}\right] \times 100 \quad (1)$$

Study of in-vitro Release Profile of Different Prepared Nystatin Spanlastics. Nystatin Spanlastical vesicles of one mL of each formula were isolated and washed using ultra-cooling centrifugation by the same previously mentioned steps, then diluted in phosphate buffer of pH 6.8, forming one mL suspension (theoretically equivalent to 5000 IU Nystatin).[16] The percent of drug released from each suspension was measured using the modified USP dissolution apparatus II (Diss 6000, Switzerland) (where one smoothly cut and open-ended 10 mL syringe tube was attached individually to each paddle and covered on the bottom with a pre-soaked cellulose membrane of 0.45 µm pore size to act as a donating vesicle) as reported in El-Hadidy GN et al.[17] The receiver vessel contained 100 mL of phosphate buffer with 6.8 pH at 37 ±0.5°C, and the paddle speed was 50 rpm.[18]

Aliquots of one mL were withdrawn at predetermined intervals over 30 minutes at 5, 10, 15, 20, 25, and 30 minutes and immediately replaced with a fresh release medium.[16,19–22] The withdrawn aliquots were then spectrophotometrically analyzed at the predetermined λ_{max} of Nystatin in a 6.8 pH (279 nm) phosphate buffer to determine the released drug amount in each time interval. The results provided are the mean values of three runs ±SD. A cumulative correction factor was applied to compensate for diluting the samples in all processes.[23,24] The results were interpreted using the (Design Expert-13) program.

Determination of Particle Size (PS), Polydispersity Index (PDI), and Zeta Potential (ZP). The average diameter in (nm), zeta potential, and polydispersity index of the prepared Nystatin Spanlastics were measured by Malvern Zetasizer at 25°C, backscatter detection of 173°C, and refractive index of 1.330 (Malvern Instruments, Ltd., UK). The preparations were appropriately diluted with distilled water that provided suitable vesicle scattering intensity to measure the size of the vesicles. The PDI was measured through dynamic light scattering (DLS), which detects the vesicle distribution. The ZP was carried out in distilled water by recording the electrophoretic mobility of charged vesicles in an electrical field and that detects the vesicle permeation behavior via studying its colloidal property and stability.[25–27] The results are the mean values of three runs ±SD. The optimal formulae were selected to be examined for their in-vitro antifungal activity.

Statistical Evaluation of the Prepared Nystatin-Loaded Spanlastics and Selection of the Optimum Formulae

All results are presented as mean (± the standard deviation) and were statistically analyzed using the Design Expert-13® software (Stat-Ease, Inc., Minnesota, USA). As mentioned earlier, the Spanlastics' formulation process was designed using that program, with 2^3 design where four center points were added to the study design to confirm the non-significance of curvature of the selected models.[27]

The results of the characterization parameters as EE%, Q30 min release percent, vesicle size, zeta potential, and PDI were modeled and analyzed by one-way analysis of variance (ANOVA); the differences within each model were considered significant when $P \leq 0.05$.[28,29] Then, a numerical optimization was performed according to the selected models to select the optimum formulae to be in-vitro evaluated for their antifungal activity.

Study of the in-vitro Antifungal Activity of the Optimized Nystatin Spanlastical Dispersions. The agar well diffusion assay method was used to assess the in-vitro antifungal activity of the top two optimum Nystatin-loaded Spanlastic formulae by measuring the induced inhibition zones.[30]

A sterilized cotton swab was used to smear a small amount of the fungal suspension of Candida Albicans (ATCC10231) of 1.4×10^6 CFU/mL concentration on (Sabouraud dextrose agar, pH 5.6 at 37°C). The Candida suspension inoculum was standardized using the 0.5 McFarland standard. Then, an equal volume of the required treatments was added individually to each well, allowing them to diffuse into the agar.

The examined treatments were the two optimum Spanlastical preparations (SP3, SP6) (equivalent to 1 mg/mL, ie, 5000IU potency/mL) and the marketed oral suspension formula (Nystatin) in three different concentrations A, B, and C (20, 1, and 0.5 mg/mL, equivalent to 100,000, 5000, and 2500 IU potency/mL, respectively). Also, the blanks of the selected preparations (SP3, SP6) were examined as negative controls.

The diameters of the formed inhibition zones were observed and measured after 24h culture at 37°C. The results were the mean values of three trials ±SD.[31,32] The Nystatin Spanlastical formula of the highest inhibition zone was statistically compared to the marketed oral suspension (Nystatin) in its three examined concentrations. After that, it was chosen to be incorporated into the solid candy preparations. Pairs of groups were compared by performing a Student's *t*-test, and multiple group comparison was conducted by the one-way analysis of variance (ANOVA) using the statistical (MS Excel, 2010) software. Differences were considered significant when $P\leq 0.05$.[28,29]

Nystatin Spanlastical Hard Candy Lozenges

Formulation of Nystatin Spanlastical Mucoadhesive Lozenges. Precisely 0.5 mL of the optimized Nystatin Spanlastic formula SP3 (equivalent to 2500 IU Nystatin), composed of Span 80 and SDC, was incorporated in each hard mucoadhesive lozenge. Four batches of Nystatin Spanlastical hard candy lozenges were formulated by 2^2 full factorial design using the corn syrup and xanthan gum amounts as independent variables at two levels, as shown in Table 3.

Batches of sixty lozenges were manufactured via the heating and congealing method.[33] In this method, sugar syrup was prepared by dissolving the required amount of sugar in a small amount of water, then warmed to (110 °C) over a paraffin bath till the sugar dissolved and gave a clear, thick syrup. The formed sugar syrup was heated to 160°C till the color changed to golden yellow. Then, the syrup was left to settle to decrease its temperature to about 90°C. After that,

Table 3 The Independent Variables' Levels Used to Formulate Nystatin Spanlastical Solid Candies by 2^2 Full Factorial Design

Factors (Independent Variables)	**Levels**	
X1: Corn syrup amount	400 mg	600 mg
X2: Xanthan gum amount	Nil	250 mg
Responses (Dependent Variables)	**Desirability Constraint**	
Y1: Drug content	Maximize	
Y2: In-vitro release %	Maximize	
Y3: Diameter	In Range	
Y4: Thickness	In Range	
Y5: Weight variation	In Range	
Y6: Surface pH	In Range	
Y7: Hardness	In Range	
Y8: Friability	In Range	
Y9: Swelling index	Maximize	
Y10: Mucoadhesive strength	Maximize	

Table 4 The Composition of the Nystatin Nano-Spanlastical Hard Candies According to the Selected 2^2 Factorial Design

Ingredients (mg)	SP3L1	SP3L2	SP3L3	SPL4
Nystatin Spanlastical dispersion*	350	350	350	350
Sugar	1400	1400	1400	1400
Corn Syrup	600	600	400	400
Beta-cyclodextrin	100	100	100	100
Acacia	200	200	200	200
Mannitol	300	300	300	300
Microcrystalline cellulose	10	10	10	10
Xanthan gum	250	Nil	250	Nil
Orange oil flavor	Q.S.	Q.S.	Q.S.	Q.S.
Orange Color (Sunset yellow FCF E110)	Q.S.	Q.S.	Q.S.	Q.S.
Total weight	3210	2960	3010	2760

Note: *0.5 mL of the Nystatin Spanlastical dispersion weighs about 350mg, with a potency of (2500 IU).

the other ingredients, such as β-cyclodextrin, mannitol, acacia, xanthan gum, corn syrup, microcrystalline cellulose, coloring agent (Sunset yellow FCF E110), and flavoring oil were added with the required amounts as mentioned in Table 4. As the melt temperature decreased to about 40 °C, the required volume of Nystatin Spanlastical dispersion was added to the mixture. Each medicated melt was then homogenized, evenly filled in sunflower oil-lubricated rubber molds, and allowed to cool at room temperature.[34] Each mold contained 20 round cavities of 9 mm depth and 20 mm diameter with a projection in the middle. Finally, the prepared lozenges of each batch were enclosed individually in an aluminum foil and kept inside a desiccator to prevent moisture uptake till the evaluation time.[35] In the method selected, sugar is considered the main base of the prepared lozenges as it helps in forming a crystalline structure that supports the lozenge's integrity during storage and use. Corn syrup was used as a sweetener and binding agent to prevent sugar crystallization, and it also helps maintain the prepared lozenges' transparency and smoothness.[36] Acacia was also used as a binding agent.[37] Beta-cyclodextrin is generally used to enhance drug mucosal penetration and to relieve pain, inflammation, and fever.[38,39] This could be advantageous for relieving the pain accompanied by oral candidiasis. Mannitol was used as a diluent that can give a cooling sensation in the mouth. Microcrystalline cellulose is also used as a diluent and disintegrant. Xanthan gum is a hydrophilic polymer used as a whipping agent.[35] Sunflower oil was used as a lubricant. Orange fruit oil flavor and orange color were added to each formula to match the preparations' taste and appearance.[40]

Characterization of the Prepared Nystatin Spanlastical Hard Candy Lozenges

Visual Inspection. All the prepared lozenges were visually inspected for their color uniformity, shape, texture, odor, and taste.

Diameter and Thickness Measurement. The diameter and thickness of the prepared lozenges of each batch were measured using a Vernier caliper, and the results were presented as the mean of six determinations ±SD.[41]

Weight Variation. Each batch's lozenges were weighted individually, and the average weight was recorded. Each lozenge weight was compared to the average value. The weight uniformity was measured according to USP specification; each result was the mean of six determinations ±SD.[42]

Surface pH Study. The pH of each formula should be measured to ensure that it falls in the salivary pH range (6.5 to 7.5) and is not irritant to the oral cavity. Each lozenge was soaked in 1 mL of warm distilled water for 2 hours to swell.

Then, the pH electrode was placed near the surface of the lozenge for one minute. Each pH result was the mean of six determinations ±SD.[43]

Hardness. The lozenges' hardness was determined using the Monsanto Hardness tester, and the force required to break each formula was noted. All the lozenges should fall within the in-house hardness range of 6.8 kg to 15 kg, and the hardness of each batch was the mean of six determinations ±SD.[44]

Friability. The friability of the lozenges was determined using the Roche Friabilator. Six pre-weighed lozenges per batch were placed in the friabilator and operated for 4 min at 25 rpm. The lozenges were then brushed carefully to free them from dust and reweighed; the friability Percent should be at most 0.8%. The friability percent of each batch was calculated using the equation provided.[43]

$$F\% = \frac{Wi - Wf}{Wi} \times 100 \tag{2}$$

W_i is the initial weight, and W_f is the final weight of the lozenges before and after the friability test.[44]

Swelling Index Studies. The swelling property of any buccal formulations is essential for proper mucoadhesion.[45] In Petri dishes containing 1% agar gel, six lozenges of each batch were weighed and placed on the surface. Each petri dish had four lozenges inside; dishes were incubated at 37 ±1 °C for one hour. After one hour, the excess water on the surface of the lozenges was removed gently using a filter paper with no pressing and then reweighed. The swelling index was calculated using the following formula:

$$\text{Swelling index} = \frac{WF - WI}{Wi} \times 100 \tag{3}$$

where W_i and W_f are the lozenges' initial weight before swelling and final weight after swelling, the result of each batch was the mean of six determinations ±SD.[46]

Determination of Mucoadhesion Strength of Nystatin Spanlastical Mucoadhesive Buccal Lozenges. The test was performed in warm conditions using a laboratory-adjusted balance by putting a 250 mL beaker on the balance's right hand. A 100-gm weight was hung on the left hand using a thin steel string. The balance was then equalized by resting the hanged weight on the base of a 250 mL inverted beaker placed inside a 500 mL beaker containing phosphate buffer of pH 6.8. The buffer amount was adjusted to reach the mucosal surface, and the temperature was kept at 37 °C. Two slices of rabbit's small intestine were cleaned with normal saline. The first was attached to the base of the 100gm weight, while the other was fixed on the bottom base of the inverted 250 mL beaker using cyanoacrylate adhesive. The lozenges were individually smoothly crushed, placed between the two mucosal sections, and left for five minutes to ensure the desired contact. An infusion device was used to drop water into the beaker on the right side at a flow rate of 13–15 drops per minute. The weight of the beaker would keep increasing till the two slices on the other side were just detached. The weight of the collected water was recorded to indicate the detachment stress (dyne/cm^2) using the following equation. The results are the mean values of six determinations ±SD.[16]

$$\text{Detachment stress}\left(\text{dyne}/\text{cm}^2\right) = (\text{m} \times \text{g}) / \text{A} \tag{4}$$

where (m) is the weight of water, (g) is the acceleration due to gravity taken as 981 cm/sec^2, and (A) is the area of the rabbit's small intestine (area of contact). The experiment was performed at room temperature in triplicates.[47,48]

Drug Content. Lozenges of each formula were weighed individually and crushed in a mortar. The crushed lozenges were soaked in 100 mL phosphate buffer pH 6.8 with considerable agitation to extract the drug. The drug content was determined spectrophotometrically at 279 nm with a blank lozenge extract as a reference. The Nystatin content results were the average of six lozenges per batch.[43]

Study of the in-vitro Release Profile of the Different Prepared Mucoadhesive Nystatin Spanlastical Lozenges

The drug release profile of each batch was studied using the USP dissolution apparatus II (paddle type) (Diss 6000, Switzerland), where accurately weighed lozenges of each batch were placed in 100 mL phosphate buffer for 30 minutes with the same temperature and agitation conditions that were used for studying the in vitro release profile of the

Spanlastical dispersions.[49] The samples were collected at the same time intervals, ie, after 5, 10, 15, 20, 25, and 30 minutes, and were immediately replaced with a fresh release medium.[16,19–22] Aliquots were filtered through the Whatman filters (0.45 μm) and analyzed using a UV spectrophotometer at 279 nm. Six lozenges of each batch were examined, so the results at each time interval were the mean of six determinations.[19] A cumulative correction factor was applied to compensate for diluting the samples in all processes.[23,24] The results were interpreted using the (Design Expert-13) program.

Statistical Analysis of the Results of the Prepared Spanlastical Lozenges and Selection of the Optimum Formula

All results were presented as (mean ± standard deviation) and were statistically analyzed using the Design Expert 13® software. The Spanlastical lozenge batches were formulated according to 2^2 design, as center points were added to confirm the non-significance of curvature of the examined models.[27]

All characterization results, such as diameter, thickness, weight, surface pH, drug content, hardness, friability, swelling index, Q30 min release percent, and detachment force, were statistically analyzed by the one-way analysis of variance (ANOVA) to check their significance. The differences within each model were considered significant when $P \leq 0.05$.[28,29] Then, a numerical optimization was performed to select the optimum formula. The batch that showed the most significance was evaluated by FTIR analysis, followed by an in-vivo antifungal activity study on rats.

Fourier-Transform Infrared (FTIR)

Using the FTIR Spectrophotometer (FTIR-8300, Shimadzu, Japan), a spectral analysis of both the pure drug alone and the physical mixture of the drug with the optimum formula's excipients (in a ratio of 1:1 per component) was performed to find out whether there were any interactions between Nystatin the drug and the used excipients.[50] The samples' scanning range was between 4000 cm^{-1} to 400 cm^{-1}.

In-vivo Antifungal Study on Rats

The Design of the Animal Experiment. Twenty-four healthy Male Wistar-type rats with an average age of 8 weeks, weighing approximately 200g, were randomly allocated to one of the four groups of equal sizes (ie, six rats in each group) using the parallel experimental design. All animal treatments and laboratory procedures were conducted according to the Egyptian National Laboratory Animal Centre regulations and approved by the Ethics Committee of the Faculty of Pharmaceutical Sciences and Drug Manufacturing (Misr University for Science and Technology, Cairo, Egypt) for 2022 with (PI06) code. Rats of all groups were kept in spacious cages. Twelve hours of light and twelve hours of darkness were set as photoperiods daily. The ambient temperature was maintained at 21°C at all times. Ad libitum access to food and water was provided for all rats. Food composition was comprehensive, balanced, and free of antifungal components throughout the entire study.[51]

Induction of Oral Candidiasis in Rats. A single colony of Candida Albicans standard opportunistic strain (ATCC10231) was isolated and cultivated on Sabouraud dextrose agar (SDA) and was grown for 18 hours at 30°C in yeast extract-peptone glucose medium YPG: (yeast extract, 2%; bacto peptone, 1%; glucose, 2%) using a shaker. Then, centrifugation was applied to harvest the culture. Cells were isolated and washed three times in phosphate buffer saline (PBS) and adjusted to a concentration of 3×10^8 CFU/mL (using a hemocytometer chamber for counting cells). Quantitative cultures of ten-fold serial dilutions on Sabouraud dextrose agar plates were used to confirm the viability of the inoculum.[52] According to Martinez et al, the oral candidiasis model was attained using immunosuppressed rats to enhance the infection rate.[53,54] The study was conducted over three consecutive weeks; in this period, eighteen rats were immunosuppressed with dexamethasone and treated with Tetracycline, while the remaining six rats were left healthy and completely normal. In the first week (one week before starting the induction of the infection), eighteen rats received 0.5 mg/L dexamethasone and 0.1% of Tetracycline in their drinking water.[53,54] On the eighth day (the first day in the second week of the study), rats received a higher dose of dexamethasone equivalent to 1 mg/L and a smaller dose of Tetracycline to 0.01% in their drinking water (and that was applied and maintained throughout the experiment), in addition to being orally infected for three days with 48h time intervals (ie, Days 8.10 and 12) by 0.1 mL of saline suspension containing ($3x10^8$ CFU/mL) twice a day. Just

before the start of the fungal inoculation, the animals were sampled to ensure that C. albicans were absent in their oral cavity. The infection was spread into the rat's oral cavity by rolling a cotton swab with Candida suspension over all parts of the mouth. Seventy-two-hour post the last inoculation (ie, Day 14), samples were collected from all subjects using the same cotton swab rolling method to confirm the presence of the fungi and also to determine the quantity and the number of Candida viable cells in their oral cavity before the beginning of the treatment process.[52,55]

Antifungal Treatment. Three days post-infection (ie, Day 15), the infected animals (n=18) were randomized into three groups (each of 6 rats), while the fourth group (n=6) was composed of the normal rats. Each group received a different treatment twice daily for seven consecutive days (from day 15 to day 21). Rats of the first group (Gp1) (n=6) were treated with the optimal Nystatin Spanlastical lozenge (SP3L1) by the topical spreading of its finely crushed sticky powder on the tongue of the rats twice a day with weights equivalent to (0.3 mg Nystatin/dose. The rats of the second group (Gp2) (n=6) were treated with the market oral suspension (Nystatin®) by applying the suspension with the exact dosing quantity and regimen protocols over the rat's tongues. The rats of the third group (Gp3) (n=6) were used as a positive control as they were infected but not treated animals. Instead of the antifungal therapy, they received an equivalent volume of sterile saline orally twice daily (0.8% agar was added to the used saline doses to increase viscosity and residence). The fourth group (G4) (n=6) animals were utterly normal, received the same saline/agar liquid volumes, and were used as a negative control.[54]

Microbiological and Histopathological Evaluation. On day 22, ie, 24 hours after the administration of the last treatment dose in each group, an overdose of ethyl urethane was used to sacrifice animals.[56,57]

The rats' tongues were morphologically and visually examined for any inflammatory or infectious signs, then removed and carefully divided into right and left sections along with each side's cheek.[58]

The right section of each tongue, along with the right cheeks, was used to conduct the microbiological study as they were suspended in 5 mL of normal saline and homogenized for 10 minutes in 25,000 RPM (Omni homogenizer GLH 02, Omni, Inc., USA). One mL of each homogenate was then subjected to tenfold serial dilutions and then evenly smeared on the Sabouraud Dextrose agar (SDA) plates.[52,54] All plates were incubated for 24 hours at 30°C to enhance the microbial growth, and then a quantitative assessment was performed by counting the colony-forming units (CFU). The log of the colony-forming units per mL (CFU/mL) was calculated to determine the number of viable cells.[52] The results of each group were statistically analyzed by the one-way analysis of variance (ANOVA) using (MS Excel, 2010) software, and differences were considered significant when $P \leq 0.05$.[28,29,59]

The left sections of each tongue, along with the left cheeks of the rats of the first and second groups (that were treated with both the SP3L1 and the market formula), were used to conduct the histopathological examination to identify inflammation or any other pathological changes that may be associated with infection.[60]

The selected tissues' specimens were fixed in 10% neutral buffer formalin, trimmed, washed in water, dehydrated in ascending grades of ethyl alcohol, cleared in xylene, and embedded in paraffin. Thin sections of (4–6μ) were processed and stained with hematoxylin-Eosin and the Periodic Acid-Schiff stain (PAS). Each section was photomicrographed using a Light microscope with magnification power of 400X and 100X (BX53; Olympus Corporation, Tokyo, Japan).[61]

Results and Discussion

Evaluation of Nystatin Medicated Spanlastical Dispersions

Visual Inspection

The prepared Nystatin Spanlastical dispersions were yellowish due to the color of the Nystatin raw material itself. All the preparations were dispersions with an accepted odor and were easily dispersed upon shaking; the turbidity was medium (++) for (SP1, SP2, SP5, and SP6) which were prepared using Span 60, while turbidity was heavy (+++) for (SP3, SP4, SP7, and SP8) that was prepared using Span 80. Those findings may be due to the Span type itself as Span 80 has a slightly lower HLB value (around 4.3) compared to Span 60 (approximately 4.7); this decrease in the HLB value can result in the formation of less stable dispersions, and a kind of phase separation can occur, and thus increased turbidity.[62]

Determination of Entrapment Efficiency (EE%)

The entrapment efficiency ranged between 95.4% ±0.27 and 99.83% ±0.039; those results could be due to the vesicle former type used (Span type), the type of the Edge activator, or the bath ultrasonication time. As shown in Figure 1, all the preparations had an entrapment efficiency higher than 95%. The highest entrapment efficiency was for SP6, composed of Span 60 and Sodium Deoxy Cholate, and was sonicated for 5 minutes. At the same time, SP7 was the formula of the lowest entrapment efficiency; it was composed of Span 80 and Tween 20 and was sonicated for 3 minutes. The SDC edge activator has a longer alkyl chain than tween 20 (ie, lower HLB value and lower molecular weight; the HLB values of Tween 20 and SDC were 16.72 and 16, and their molecular weights were 1225 Da and 416.6 Da, respectively), so the Spanlastics prepared using SDC showed an enhanced EE%. Using surfactants with high molecular weight as tween causes disturbance in the entity of the vesicle's bilayer membrane that enhances the drug diffusion to the aqueous medium during the centrifugation step and so reduces the (EE%) of the prepared Spanlatics.[63]

The results also showed that the type of vesicle-forming agent selected can affect the EE% of the prepared formulae. Span 80 has an extra extended alkyl chain than Spn60. It has unsaturation in its structure, so it has a low vesicle formation ability that impacts and reduces its EE%.[11,64] Consequently, the formulae of Span 60 showed higher EE% than those of Span 80. Figure 2 illustrates a 3D surface diagram of the interaction between the effect of the Span type factor and the edge activator type factor upon fixing the third factor (sonication time). Moreover, it was noticed that increasing the bath sonication time increased the EE% because of the dispersing of the nanoparticles within the surrounding medium and providing more thorough mixing.[65,66] The individual effect of each factor levels on the drug entrapment was presented in Figure 3.

Study of in-vitro Release Profile of Different Prepared Nystatin Spanlastics

As shown in Figure 4, the in-vitro drug release percent after 30 minutes ranged between 52.86 ±2.5 and 95.83 ±2.04; the maximum release percent was for SP3 (Span 80 and SDC), while the lowest release percent was for SP2 (Span 60 and tween 20). It was noticed that there is an indirectly proportional relationship between the EE% and the drug release from the prepared Spanlastics. Also, it was reported that Span80 Spanlastics showed more drug release percent than those of Span 60 due to the structure of Span 80 (extra alkyl chain and unsaturation) that reduces the tightness of the vesicle's membrane.[67] Considering the edge activator type, it was noticed that the formulae of the ideal release percent were a combination of Span 80 in addition to the SDC edge activator. SDC can significantly enhance the release characteristics of the Span 80 Spanlastics by improving the vesicle fluidity, which promotes the drug permeation process.[68]

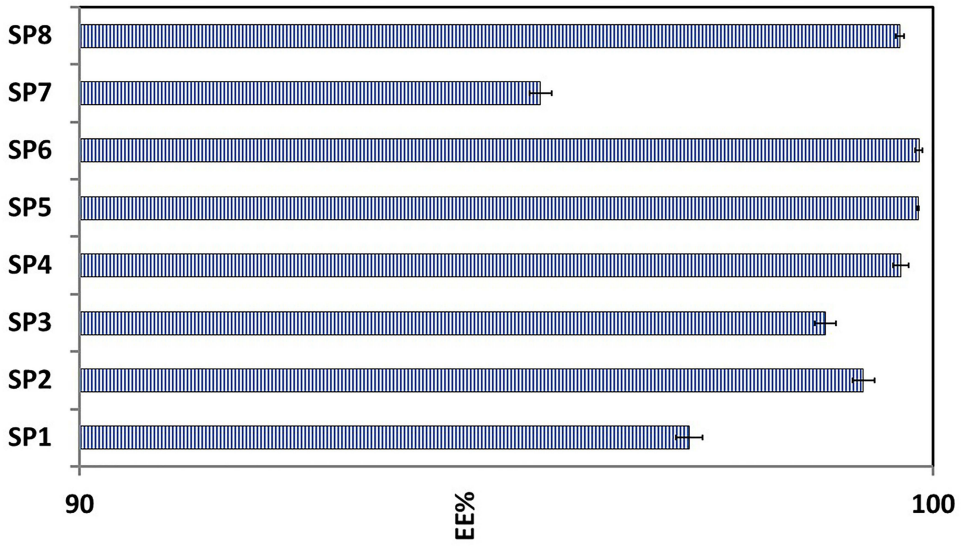

Figure 1 Entrapment percent of Nystatin loaded Spanlastics; each result is the average of three readings ±SD (n=3).

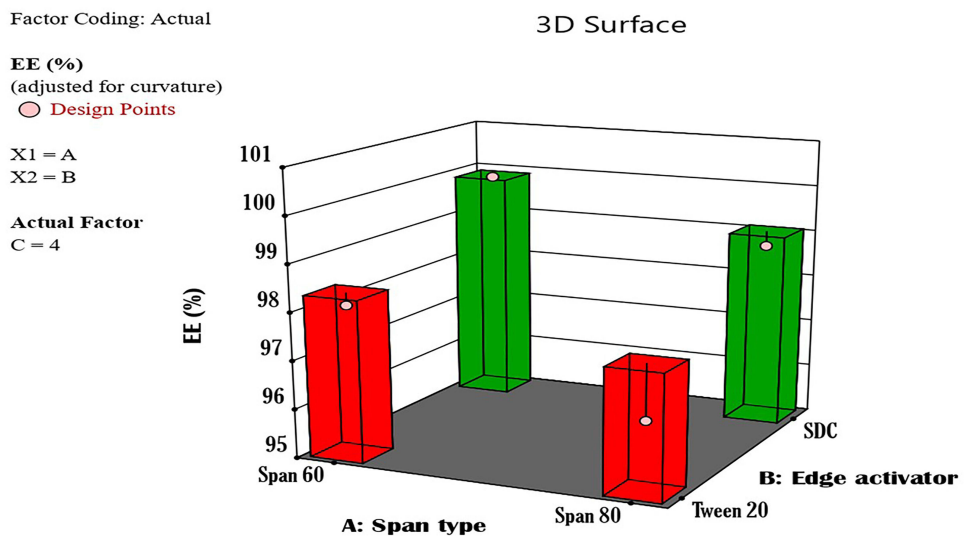

Figure 2 A 3D surface diagram of the effect of the combination of both A and B independent variables upon fixing the C variable on the entrapment efficiency of the prepared Nystatin Spanlastics where (A) is the Span type, (B) is the edge activator type, and (C) is the bath sonication time in minutes.

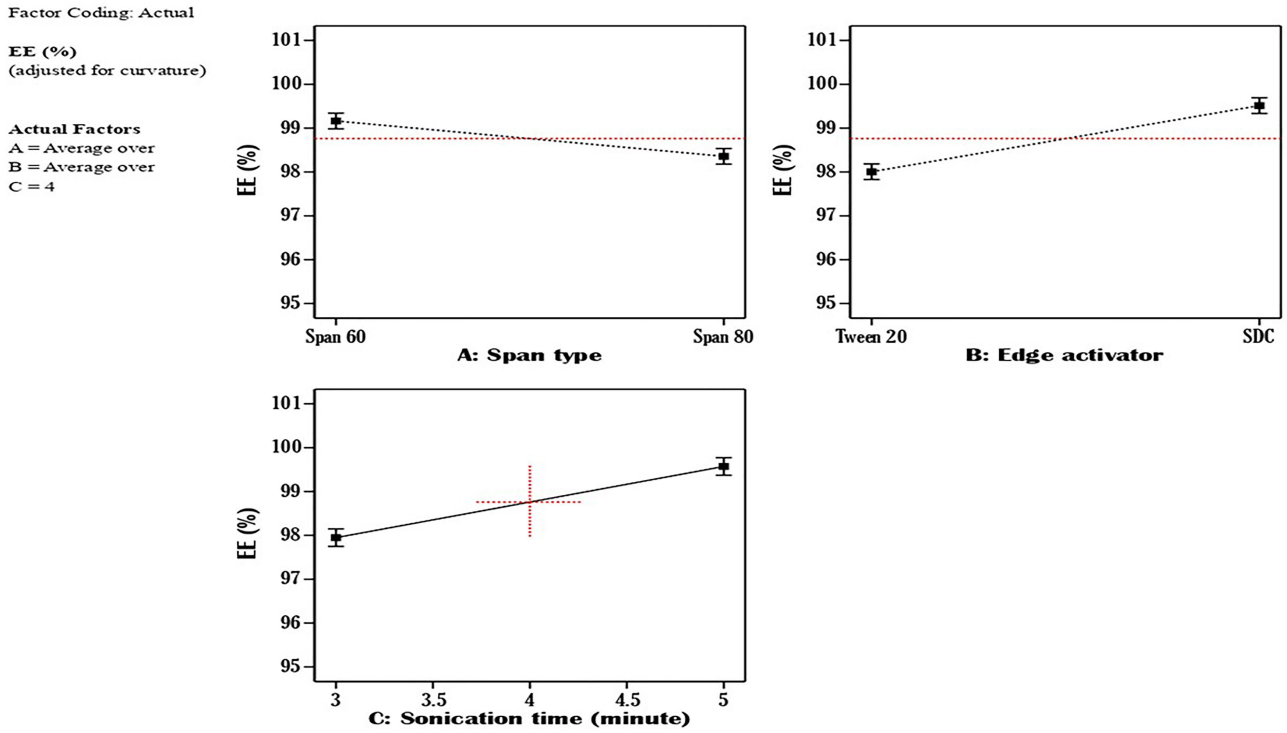

Figure 3 The effect of all factors (**A**–**C**) on the entrapment efficiency of the prepared Nystatin Spanlastics where (**A**) is the Span type, (**B**) is the edge activator type, and (**C**) is the sonication time in minutes.

On the other hand, the Spanlastics prepared by Span 80, in addition to tween 20, showed lower drug release percent. Abdelbari et al, 2021 reported that Tween 80 edge activator increased the bilayer hydrophobicity of the Spanlastic formulations due to the presence of the alkyl chain in its structure, leading to a lower drug release percent.

While there are not enough studies directly addressing the effect of Tween 20 on Span 80 Spanlastics, it is probable that Tween 20, being a structurally similar surfactant, could have a comparable impact on drug release when combined with Span 80.[69]

https://doi.org/10.2147/DDDT.S504768

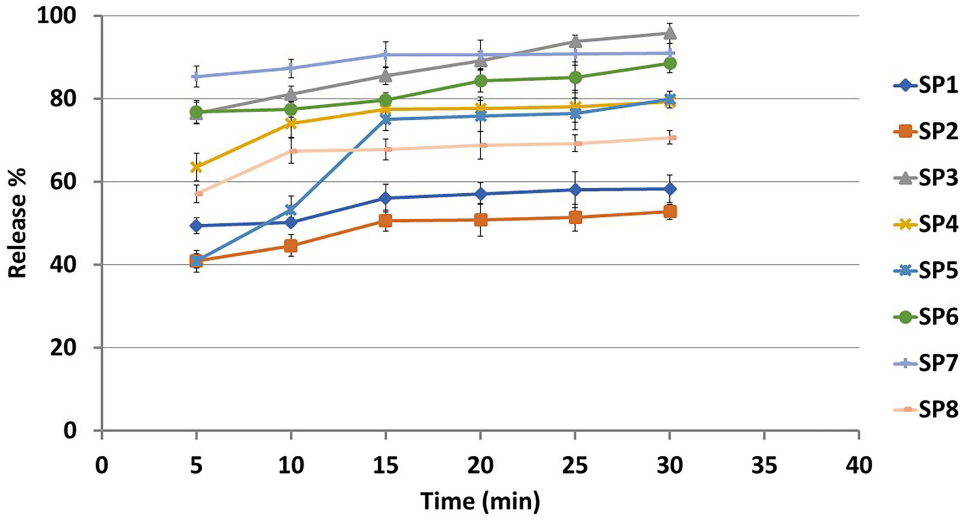

Figure 4 In-vitro release profile of Nystatin loaded Spanlastics after 30 minutes in phosphate buffer of pH 6.8; each result is the average of three runs ±SD (n=3).

Also, Mazyed et al 2021 reported that Tween 20 could somewhat enhance the drug release profile but does not disrupt the lipid structures as effectively as SDC. Its role is more about maintaining vesicle stability rather than significantly increasing drug permeability. At the same time, SDC is more effective at increasing drug release due to its superior ability to enhance membrane permeability.[62]

Figure 5 shows a 3D surface diagram of the combination effect of the Span and edge activator types on the in-vitro drug release after 30 minutes.

Regarding the sonication time, formulae sonicated for 3 minutes showed a higher drug release percent than those sonicated for 5 minutes. As the sonication time increases, the percent of the drug released decreases; that is, due to the agglomeration of vesicles, the destabilization of the system itself after excessive sonication, and the creation of a thermodynamically unstable environment that hampers drug release percent.[70] Figure 6 shows the individual effect of each factor level on the drug release percent.

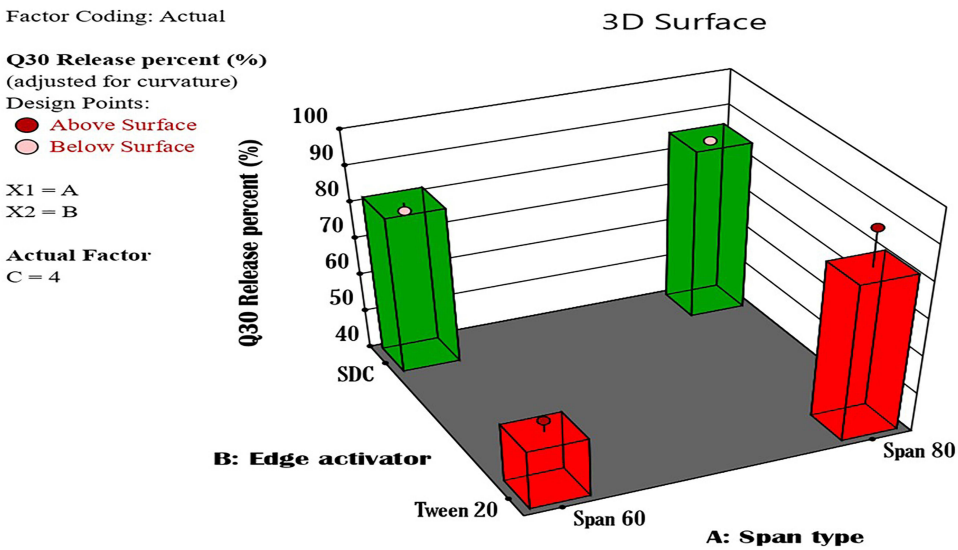

Figure 5 A 3D surface diagram of the effect of the combination of both A and B independent variables upon fixing the C variable on the in-vitro drug release of the prepared Nystatine Spanlastics after 30 minutes where (A) is the Span type, (B) is the edge activator type and (C) is the bath sonication time in minutes.

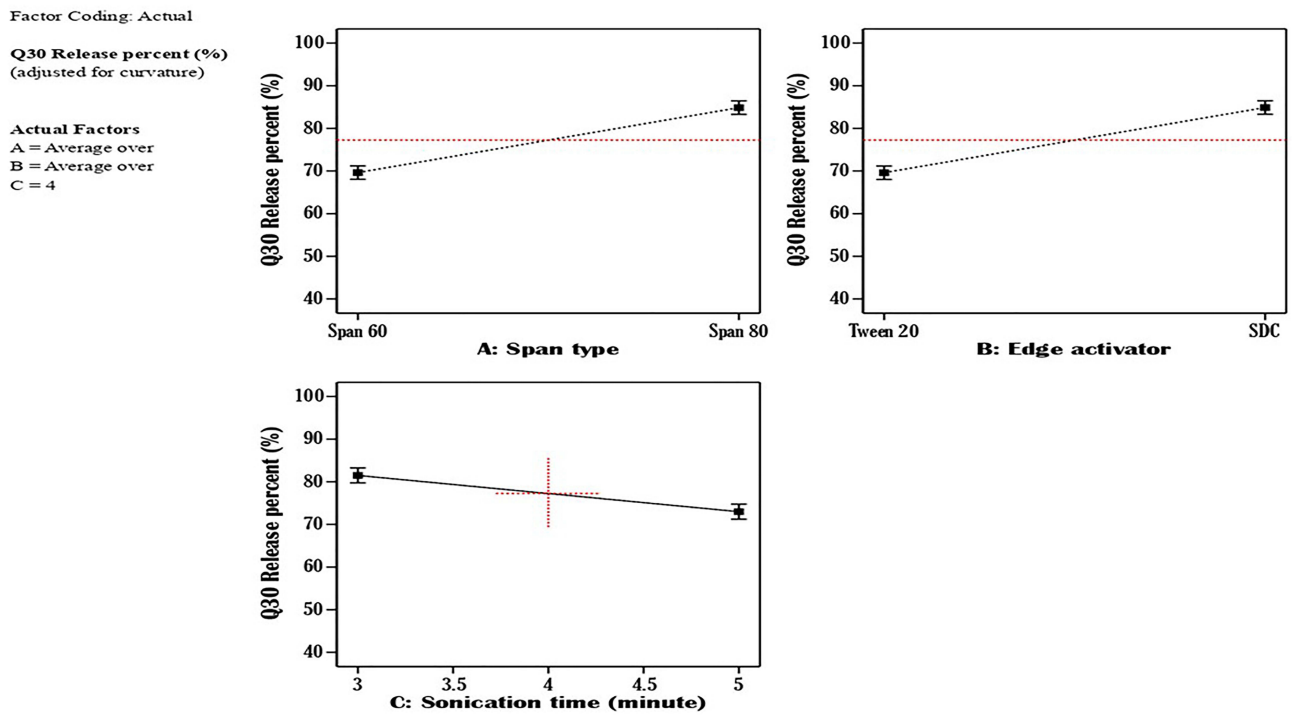

Figure 6 The individual effect of all independent variables on the in-vitro drug release percent of the prepared Nystatin Spanlastics after 30 minutes, where (**A**) is the Span type, (**B**) is the edge activator type and (**C**) is the sonication time in minutes.

Determination of Particle Size (PS), Polydispersity Index (PDI), and Zeta Potential (ZP)

The PS range in (nm) was 202.2± 10.31 to 376.7± 41.9, the PDI range was 0.259±0.022 to 0.405±0.075, and the zeta potential in (mV) was from −40.7±2.53 to −51.7±1.29; Figure 7. The most crucial factors that enable the nanocarrier vesicles to cross any biological membranes are their charge, size, and dispersity index. These factors detect the vesicle's ability to pass through the tiny pores of the biological membranes. Smaller vesicular sizes, for example, can ensure a deeper penetration of the biological barriers. Therefore, all these factors should be compromised to get the optimum vesicles.[71]

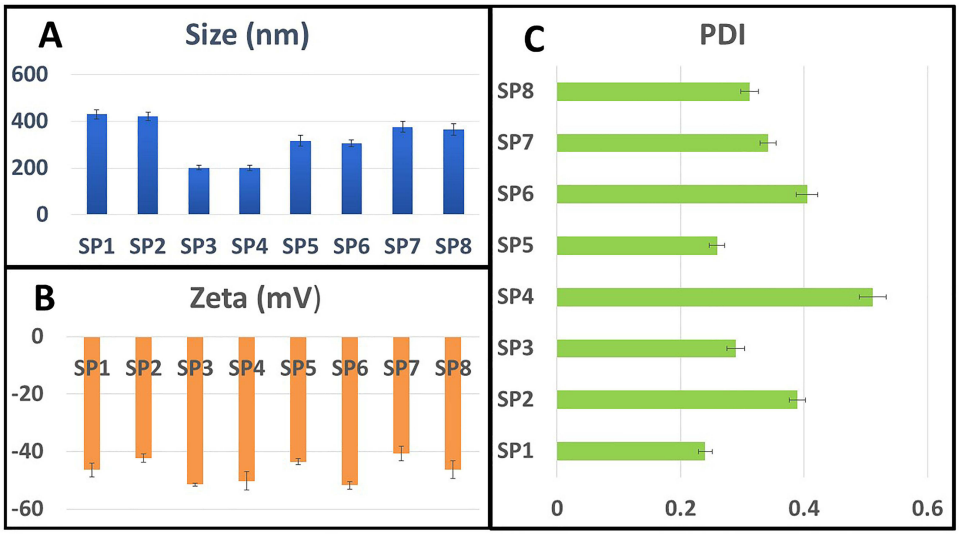

Figure 7 (**A**) Vesicle's size of Nystatin Spanlastics (PS), (**B**) Nystatin Spanlastics' zeta potential (ZP), and (**C**) Nystatin Spanlastics' polydispersity index (PDI); each result is the average of three readings ±SD (n=3).

https://doi.org/10.2147/DDDT.S504768

Spanlastics are unique carriers due to the edge activators in their composition that provide high flexibility and deformability compared to the other colloidal carriers.[72] It was noticed that the type of EA affects the vesicle size as the formulae containing the SDC edge activator in addition to Span 80 (SP3) showed a smaller vesicular size than those composed of Tween 20 in addition to the same type of Span (SP7). Using EAs as SDC with lower HLB value compared to tween 20 (ie, lower hydrophilicity) will consequently reduce the vesicle's surface energy. As a result, a smaller vesicular size is obtained,[73] as shown in Figure 8 (I).

Also, it was observed that upon fixing the edge activator type selected, Span 80 Spanlastics showed a smaller size than Span 60 preparations, which might be due to the increased hydrophobicity of Span 80 over that of Span 60. Also, the decreased surface free energy of Span 80 can cause a reduction in the vesicular size.[74]

The prolonged exposure of the vesicles to bath sonication results in small vesicular sizes.[75] The vesicular size results showed that SP6, for example, was smaller than SP5; however, both contained the same ingredients (Span60 and SDC) but were sonicated for 5 minutes and 3 minutes, respectively. Figure 9 (I) shows the effect of all independent variables on the vesicle's size.

Zeta potential and the vesicles' electrical charge affect the prepared Spanlastics' stability. If the zeta potential is between (–) 30 mV and (+) 30 mV, the dispersion system may show instability like flocculation or aggregation promoted due to Van der Waals attractions. So, the higher the ZP values, regardless of the charge, the higher the stability of the dispersions could be.[76] All the prepared Nystatin Spanlastics showed negative zeta potential values that exceed (–) 30 mV, which indicates their stability. Preparations used anionic in nature EA as SDC has a negative charge on the surface of the vesicles. Baring a negative charge is considered necessary as that enhances the vesicle's permeability by the effect of the repulsive forces between the negatively charged vesicles and the biological barrier's surface, which helps them to diffuse deeper and faster through the biological membranes than the positively charged vesicles.[77] Formulae containing non-ionic surfactants as tween 20 show a decreased negativity of the formed vesicles.[78] Figure 8 (II) shows the 3D surface diagram of the interaction effect between the Span type and edge activator type; it was found that SDC always gave higher values no matter what the Span type used was. Figure 9 (II) shows the independent factors' effect on the

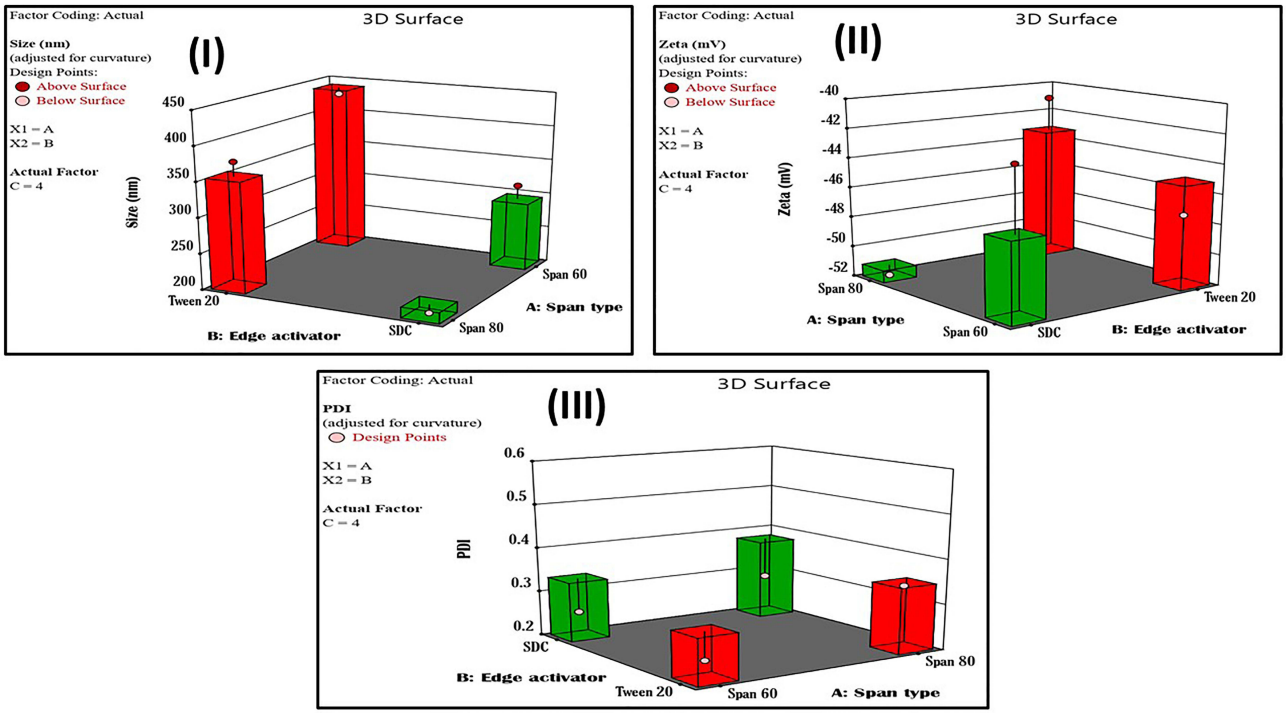

Figure 8 3D surface diagrams of the effect of the combination of both A and B independent variables on the (**I**) Nystatin Spanlastics' particle size (PS), (**II**) Nystatin Spanlastics' zeta potential (ZP) and (**III**) Nystatin Spanlastics polydispersity index (PDI) upon fixing the C variable; where (A) is the Span type, (B) is the edge activator type and (C) is the sonication time in minutes.

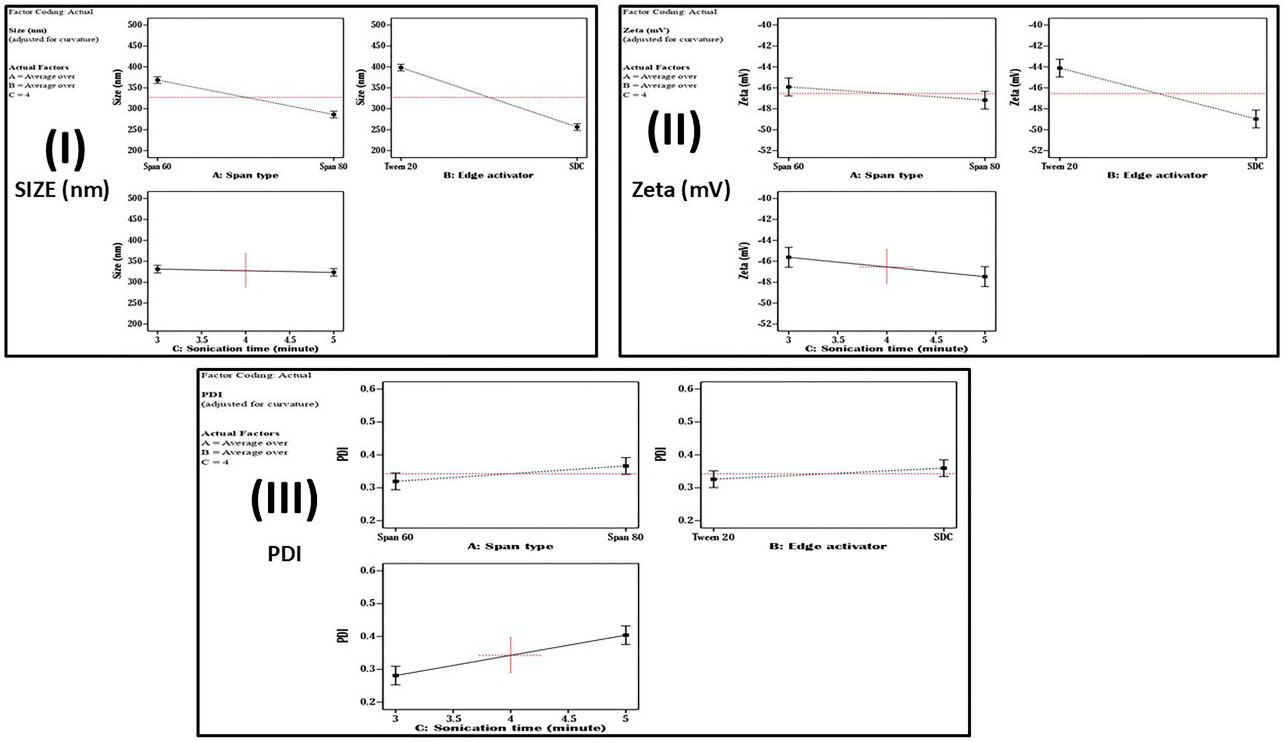

Figure 9 The effect of all independent variables on the (**I**) Nystatin Spanlastics' particle size (PS), (**II**) Nystatin Spanlastics' zeta potential (ZP), and (**III**) Nystatin Spanlastics' polydispersity index (PDI), where (A) is the Span type, (B) is the edge activator type and (C) is the sonication time in minutes.

prepared vesicle's charge. Span 80, SDC, and 5 min sonication resulted in the highest charge negativity and enhanced expected tissue penetration.

The polydispersity index (PDI) is a homogeneity indicator of the prepared vesicular dispersions. It also indicates whether there is a fair-size distribution within the formulations. The smaller the reported results (ie, approaching zero), the more homogenous the distribution is.[79,80]

Figure 8 (III) shows the interaction effect of the Span and edge activator types on the PDI values. It was found that tween 20 induced smaller PDI values with both Span 60 and Span 80.

After evaluating factors' levels individually, it was found that Span 60, Tween 20, and 3 min sonication gave the lowest polydispersity index, as illustrated in Figure 9 (III).

Statistical Analysis of the Prepared Nystatin-Loaded Spanlastics and the Selection of the Optimum Formulae

The models selected for each parameter showed significance as P values were ≤0.05. The coded equations of each model were as follows: EE% = +98.76 −0.4031A +0.7540B +0.8117C +0.3255 AC −0.5903 BC, Q30 release percent = +77.24 +7.62 A +7.64 B −4.25 C −5.74 AB −5.05 AC +2.30 BC −1.24 ABC, Size = +327.44 −41.21 A −70.98 B −3.86 C, PDI = +0.3427 +0.0235 A +0.0168 B +0.0614 C, Zeta potential = −46.54–0.6299 A - 2.43 B - 0.9249 C −1.58 AB - 0.1676 AC −0.8176 BC + 2.5 ABC, where A is the Span type, B is the Edge activator, and C is the Sonication time. The study also confirmed the non-significance of the curvature in all the selected models, as the P values were >0.05.

The numerical optimization depending on the statistical results and according to the criteria illustrated earlier in Table 1 (maximum EE%, maximum Q30%, minimum V. size (nm), minimum PDI, and maximum zeta potential (mv) as absolute value); reported that SP3 has the highest desirability (0.842), followed by SP6 (0.705); Table 5. So, SP3 and SP6 were selected to be examined for their in-vitro antifungal activity. Also, the ramps diagram that details the desirability of the most optimum Nystatin plastic formula (SP3) is illustrated in Figure 10.

https://doi.org/10.2147/DDDT.S504768

Table 5 The Numerical Optimization Report of the Most Desirable Nano-Spanlastic Formulae

No.	Span Type	EA	Sonication Time	EE%	Q30 Release Percent	Size	PDI	Zeta	Desirability	Status
1*	**Span 80**	**SDC**	**3.000**	**98.671**	**94.992**	**219.110**	**0.322**	**−51.802**	**0.848**	**Selected**
2**	**Span 60**	**SDC**	**5.000**	**99.920**	**87.350**	**293.795**	**0.398**	**−50.859**	**0.705**	**Selected**
3	Span 80	Tween 20	4.916	99.283	73.462	353.680	0.406	−45.723	0.471	
4	Span 80	Tween 20	4.904	99.261	73.590	353.728	0.405	−45.688	0.471	
5	Span 80	Tween 20	4.891	99.238	73.719	353.776	0.404	−45.654	0.471	
6	Span 80	Tween 20	4.866	99.192	73.979	353.873	0.402	−45.583	0.471	

Note: 1* is the SP3 formula, and 2** is the SP6 formula.
Abbreviations: EA., Edge activator; SDC, Sodium deoxy Cholate; EE, Entrapment efficiency; PDI, Poly dispersity index.

Determination of the in-vitro Antifungal Activity of the Optimum Nystatin Spanlastical Dispersions

Figure 11 shows the inhibition zones that were induced by the examined treatment. It was found that SP6 gave the largest inhibition zone (32 mm ±0.2); however, its blank also showed a large inhibition zone of (21 mm ±0.5) which may reflect an antifungal activity of Span 60 itself.[81] To detect the Nystatin's actual antifungal activity in that preparation (the real inhibition zone induced by the Nystatin pure drug itself), we subtracted the inhibition zone of SP6 blank from that of the SP6 formula. Then, the actual inhibition zone diameter was 11mm. On the other hand, the SP3 formula showed an inhibition zone diameter of (26 mm ± 0.7) and no activity appeared with its blank. As a result, the net inhibition diameter gained by Nystatin was 26mm. These findings directed the focus to the SP3 formula as its components enhanced the Nystatin activity the most. The inhibition zones induced by the different concentrations of the marketed oral suspension (Nystatin) gave lower inhibition zones than those of both SP3 and SP6. All results are reported in Table 6. This examination confirmed that the prepared Nystatin Spanlatics (Sp3 and Sp6) of the 5000 IU/mL potency have more

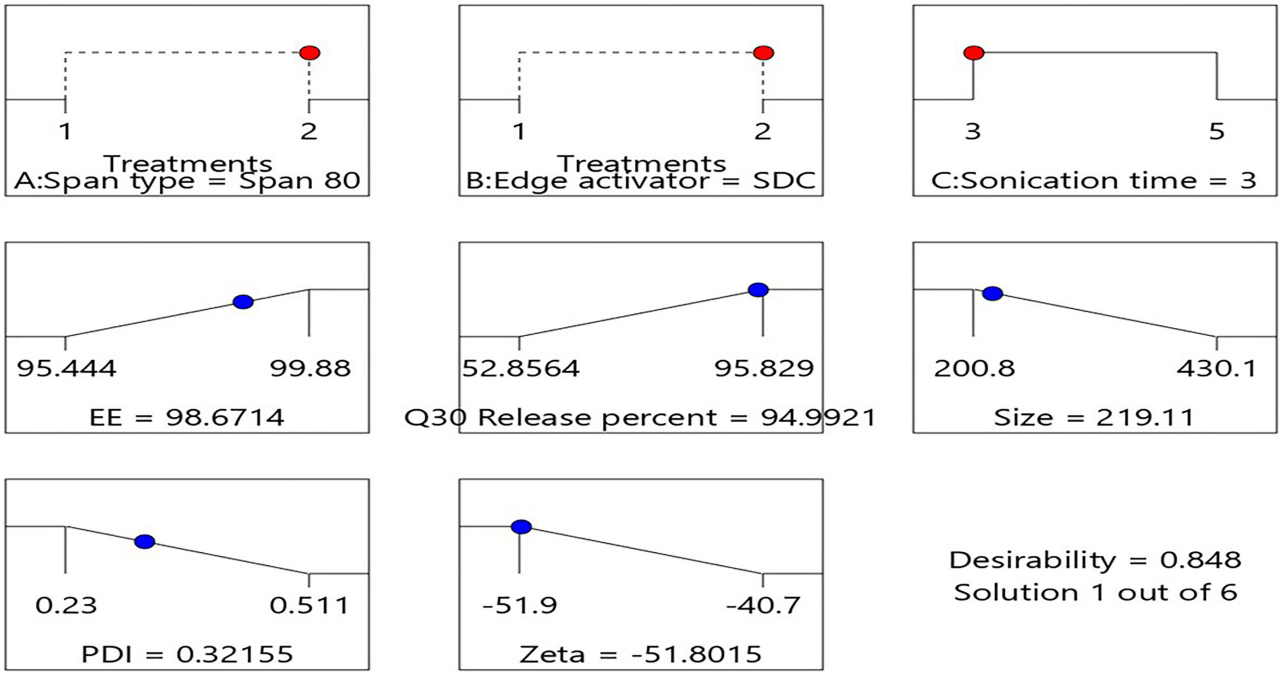

Figure 10 The numerical desirability ramps diagram of the optimum Nystatin Spanlastic formula (SP3).

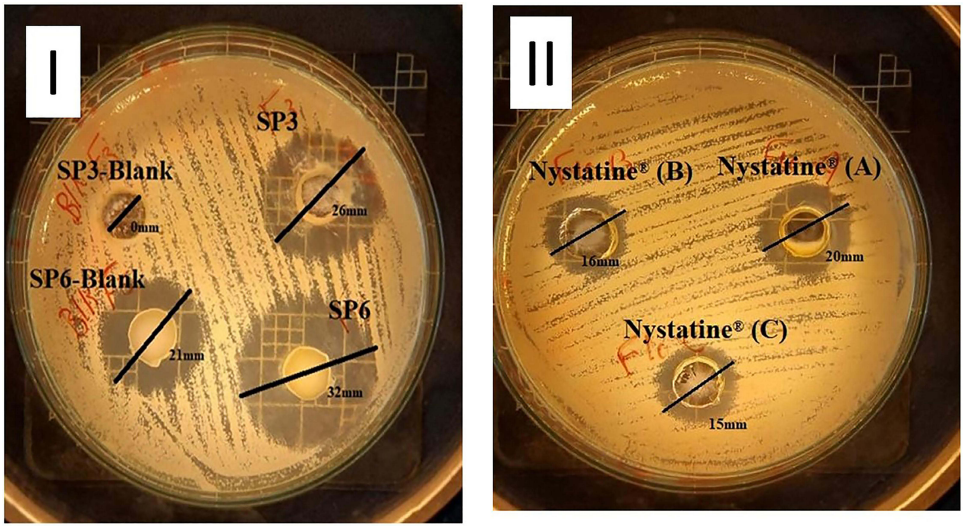

Figure 11 (**I**) The in-vitro antifungal activity (inhibition Zones) of the selected Nystatin Spanlastical dispersions SP3 and SP6 1 mg/mL (5000IU/mL) along with their blanks, (**II**) The in-vitro antifungal activity (inhibition Zones) of the Marketed oral suspension Nystatin® with three concentrations (A) Original concentration 20mg/mL (100,000 IU/mL) (B) dilution of 1 mg/mL (5000 IU/mL) (**C**) dilution of 0.5 mg/mL (2500IU/mL).

activity even than the marketed formula that contains 100,000 IU/mL potency, ie, this approach successfully decreased the dose about 20 times with an elevated activity. The SP3 formula (that showed the optimum in-vitro antifungal activity), when statistically compared to the different examined concentrations of the market oral suspension (Nystatin),

Table 6 The in-vitro Antifungal Activity (the Induced Inhibition Zones (Mm) of the Different Treatments as (Mean ± SD) (n=3)) and the Statistical Comparison of the Mean Inhibition Zone of SP3 and the Market Formulae Nystatin® with Its Different Examined Concentrations

Formulae	**Concentration mg/mL**	**Equivalent Potency/Ml (IU)**	**Reported Inhibition Zone (mm)±SD, (n=3)**
SP3	1	5000	26±0.7
SP3 Blank	0	0	0±0.0
SP6	1	5000	32±0.2
SP6 Blank	0	0	21±0.5
Nystatin (A)	20	100,000	20±0.1
Nystatin (B)	1	5000	16±0.2
Nystatin (C)	0.5	2500	15±0.5
Statistical comparison of the mean values of the reported inhibition zones (mm)			**Significance of difference at (P≤ 0.05)**
SP3		**(Nystatin®) Marketed oral suspension**	
26±0.7		**Nystatin (A)=** 20±0.1	S.D.
		Nystatin (B)= 16±0.2	S.D.
		Nystatin (C)=15±0.5	S.D.

Note: (A) is (Nystatin) oral suspension with the original concentration available in the market, (B) and (C) are prepared dilutions of the market formula (Nystatin).
Abbreviations: S.D., Significant difference; n, number of samples; SD, Standard deviation.

https://doi.org/10.2147/DDDT.S504768

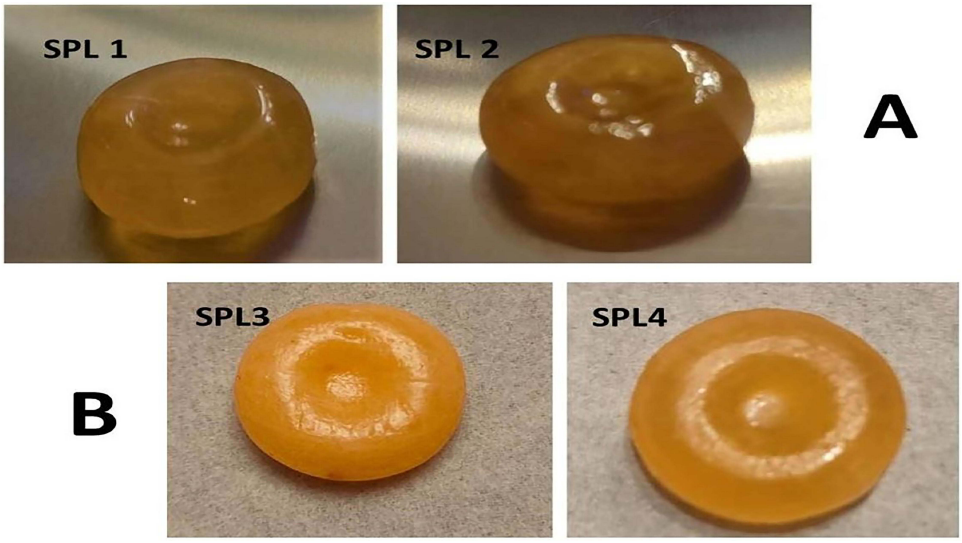

Figure 12 Nystatin Spanlastical-solid candy lozenges; (**A**) SPL1& SPL2 and (**B**) SPL3 &SPL4.

showed a significant difference at $P \leq 0.05$, as illustrated in Table 6. Therefore, SP3 was selected to be incorporated into the solid candy lozenges' preparation.

Evaluation of Nystatin Medicated Spanlastical Hard Candy Lozenges

Visual Inspection

As shown in Figure 12, the prepared lozenges of SPL1 and SPL2 had a shiny, translucent appearance, which may be due to the high ratios of corn syrup, while batches of SPL3 and SPL4 were slightly opaque. Due to the mold shape, the lozenges were round with smooth edges and a deep groove in the center. All the lozenges were orange and sticky when touched with wet hands; also, all the prepared batches had an orange Odor and a sweetened orange taste, Table 7.

Table 7 Physicochemical Properties of the Formulated Nystatin Spanlastical Solid Candies, as (Mean±SD), (n=6)

Test	Batch 1 (SPL1)	Batch 2 (SPL2)	Batch 3 (SPL3)	Batch 4 (SPL4)
Color	Orange	Orange	Orange	Orange
Shape	Round with a deep groove in the middle	Round with a deep groove in the middle	Round with a deep groove in the middle	Round with a deep groove in the middle
Taste	Sweetened orange taste	Sweetened orange taste	Sweetened orange taste	Sweetened orange taste
Odor	Orange scent	Orange scent	Orange scent	Orange scent
Diameter (mm)	19.80± 0.008	19.74± 0.011	19.78± 0.002	19.69± 0.000
Thickness (mm)	8.01 ± 0.001	7.93± 0.000	7.98 ± 0.009	7.90± 0.003
Weight (mg)	3210± 0.012	2960± 0.007	3010± 0.003	2760± 0.015
Surface pH	6.88± 0.19	6.90± 0.03	6.85± 0.12	6.92± 0.06
Drug content (%)	98.4± 0.23	99.6± 0.07	89.9± 0.05	98.1± 0.19
Hardness (kg/cm^2)	10.49 ± 0.51	9.93 ± 0.18	10.56± 2.18	10.33± 0.62
Friability (%)	0.257 ± 0.062	0.259 ± 0.028	0.248 ± 0.055	0.255 ± 0.039

(*Continued*)

Table 7 (Continued).

Test	Batch 1 (SPL1)	Batch 2 (SPL2)	Batch 3 (SPL3)	Batch 4 (SPL4)
Swelling index after 3 hours (%)	55.87± 1.18	55.90 ± 1.92	54.63 ± 0.60	55.02± 0.82
Drug Release After 30 min (%)	92.1 ± 1.2	84.4 ± 1.9	90.7 ± 0.1	83.6 ± 0.7
Detachment force (dyne/ cm^2) $\times 10^2$	243.5±2.5	318±2.9	255.4±2.9	287.8±6.4

Diameter and Thickness Measurement

The prepared lozenges were uniform, with negligible diameter variation. As shown in Table 7, the diameter of the prepared lozenges ranged between 19.69± 0.000 mm and 19.80± 0.008 mm, and the lozenge's thickness was between 7.90 ± 0.003 mm and 8.01± 0.001 mm. Due to the mold dimension restrictions, diameters were considered uniform.

Weight Variations

As reported in Table 7, the total weight of the prepared lozenges varied from batch to batch due to their composition. However, the lozenges within each batch were uniform, and their weight variations were within the acceptable range (ie, ± 5% of the batch's average weight) due to uniform mold filling.[82]

Surface pH Study

The surface pH of the prepared lozenges ranged between 6.85±0.12 and 6.92±0.06, which is considered acceptable and non-irritant to the oral cavity mucosal membrane[3] Table 7. It was noticed that the surface pH of the prepared lozenges was not much affected by the corn syrup levels but was decreased in batches of higher xanthan gum levels, as shown in Figure 13. No particular study reported that Xanthan gum itself can significantly alter the preparation's pH. However, its concentration

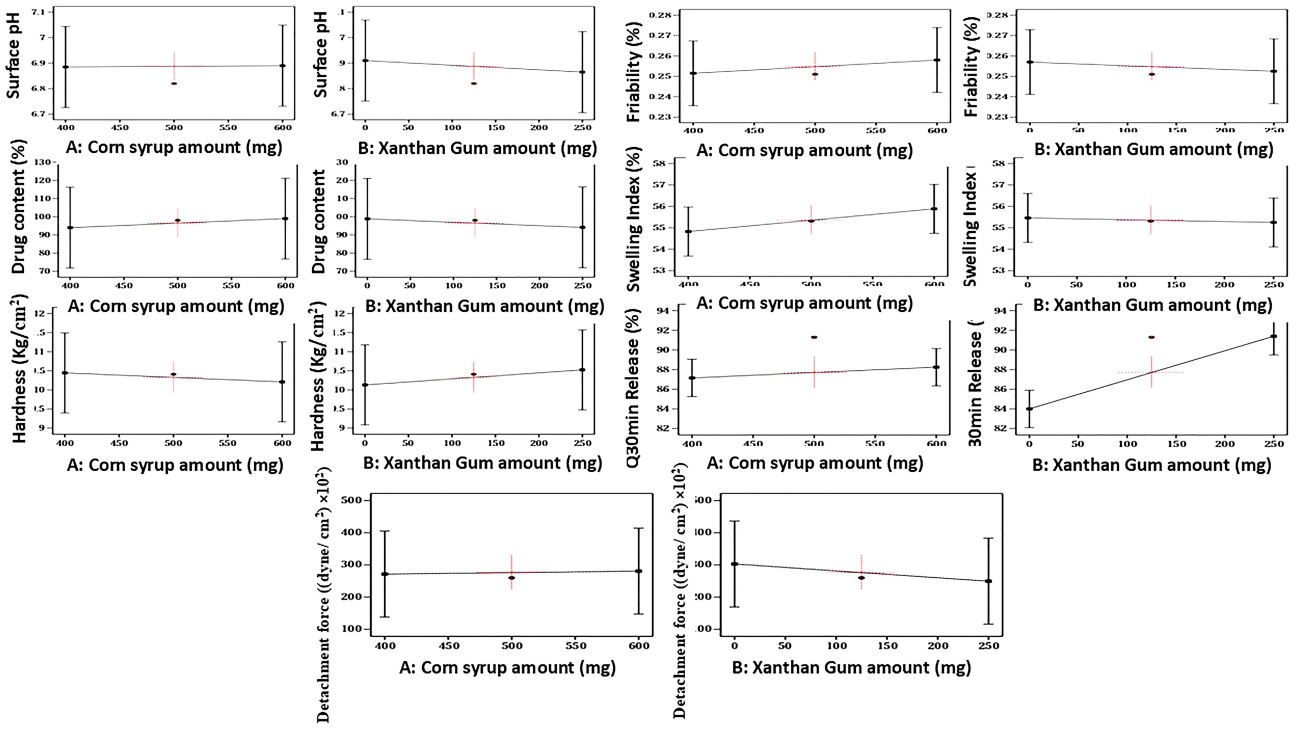

Figure 13 Effects of the high and low levels of both design's independent variables, (X1) corn syrup amount and (X2) xanthan gum amount, on the different characterization tests of Nystatin Spanlastical- solid candy lozenges, where (A) is the corn syrup amount and (B) is the xanthan gum amount.

https://doi.org/10.2147/DDDT.S504768

in lozenges can affect its viscosity in addition to the possibility of its interaction with other ingredients, which may indirectly influence the overall pH of the product.[83]

Hardness

The hardness range of the prepared batches was between 9.93 ± 0.18 and 10.56± 2.18 kg/cm2, which reflects good mechanical strength and an ability to withstand the physical and mechanical stress of handling and storage,[44] Table 7. As shown in Figure 13, the hardness of the prepared lozenges decreased with high levels of corn syrup and increased with high levels of xanthan gum.

Corn syrup is hygroscopic and, when used in high concentrations, can increase the moisture content of the lozenge's matrix, consequently reducing its hardness.[84]

At the same time, xanthan gum is a hydrocolloid that increases the lozenge's viscosity through gel formation, which can directly impact the texture and hardness of the prepared lozenge.[85]

Friability

The friability of the prepared batches ranged between 0.248± 0.055% and 0.259± 0.028%, which falls within the accepted friability range and indicates an excellent mechanical resistance of all the prepared lozenges,[43,44] Table 7. An inversely proportional relationship was found between the lozenge's hardness and friability (ie, less hardness makes the lozenges have a high liability to be highly friable).[86,87] As mentioned before, corn syrup is sticky, viscous, and hygroscopic and can attract and retain moisture in the lozenge's internal structure, which potentially reduces the lozenge's friability. It was also found that the friability decreased with higher levels of xanthan gum, as shown in Figure 13.

Swelling Index Studies

The swelling index of all prepared batches after 3 hours ranged between 54.63% ± 0.60 to 55.90% ± 1.92, indicating an acceptable wettability and good mucoadhesive properties,[46] Table 7. It was found that the swelling index of the prepared lozenges increased with higher levels of corn syrup than the xanthan gum, as shown in Figure 13. As corn syrup is hygroscopic in nature, it gives the lozenges a high ability to attract and retain water.[87]

Determination of Mucoadhesion Strength of Nystatin Spanlastical Mucoadhesive Buccal Lozenges

After testing the detachment stress of each batch, the reported results were between 243.5±2.5 and 318±2.9 (dyne/cm^2) $\times 10^2$, which indicates an acceptable residence and good mucoadhesion of the lozenges in the oral cavity even when crushed by the patient's teeth,[48,] as shown in Table 7.

Figure 13 illustrates that the prepared lozenges' mucoadhesion level is directly proportional to their swelling index. This relation may be due to the raised hydration liability, potentially influencing the interaction and adhesion between the lozenges and the oral mucosal surfaces.[88]

Drug Content

Table 7 reported that the drug content percent of all batches ranged from 89.9±0.05% to 99.6±.0.07% w/w, which does not exceed the specifications of IP 2007.[43] Also, the drug content of the prepared Spanlastical lozenges was high in the preparations of high corn syrup concentrations, as shown in Figure 13.

Study of the in-vitro Release Profile of the Different Nystatin Buccal Mucoadhesive Spanlastical Lozenges

Over 80% of the Nystatin drug was released from all batches after the 30-minute release study. The prepared lozenges showed drug release ranging from 83.6±0.7% to 92.1±1.2% by 30 minutes; Table 7. The in-vitro drug release profile of all batches over 30 min is presented in Figure 14.

Figure 13 shows that the in-vitro drug release percent of the prepared lozenges increases with the higher level of corn syrup and xanthan gum. Corn syrup is hygroscopic in nature and in high concentrations, it forms a very viscous matrix that can attract and retain water. This feature facilitates a quicker dissolution rate of the drug when the lozenge is subjected to saliva in the oral cavity, which in turn might impact the drug release characteristics.[89,90]

Xanthan gum is a hydrophilic polymer that also plays a crucial role in the drug release rate from lozenges. It increases the formulation's viscosity by forming a gel-like matrix upon hydration, which not only aids in retaining moisture but

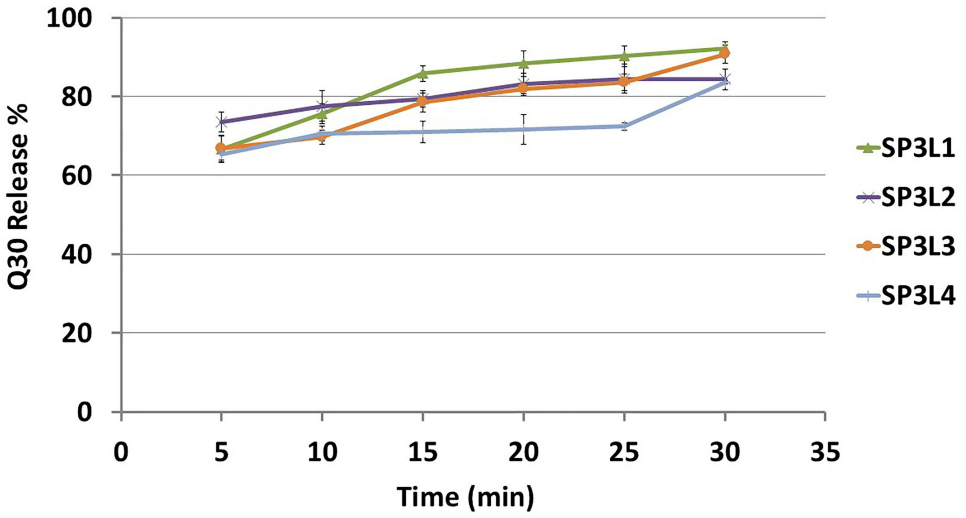

Figure 14 In-vitro release profile of Nystatin Spanlastical solid candies over 30 minutes in phosphate buffer of pH 6.8; each result is the average of 6 readings ±SD (n=6).

also enhances mucoadhesion and prolongs drug release. It can also provide a controlled release pattern by forming a gel barrier that gradually dissolves in saliva.[34] When both corn syrup and xanthan gum are used together in the lozenge formulation, their combined effects lead to an increased drug release percentage.[91]

Statistical Analysis of the Prepared Nystatin-Loaded Spanlastical Lozenges and Selection of the Optimum Batch

Upon the statistical analysis of the characterization results of the different Spanlastical lozenges, it was found that most parameters such as diameter, thickness, weight, surface pH, hardness, friability, swelling index, mucoadhesion coefficient, and drug content showed non-significant differences between batches as P values were >0.05. However, the Q30 min release percent was found to be more effective as it showed a significant difference between batches as the P value was ≤0.05. The study also confirmed the non-significance of the curvature in all the selected models, as the P values were >0.05.

The numerical optimization, depending on the statistical results and according to the criteria illustrated earlier in Table 3, reported that SP3L1 has the highest desirability (0.799), Figure 15. SP3L1 was selected to be analyzed by Fourier Transform Infrared (FTIR) to check for any possible interactions between its components and then was subjected to an in-vivo study on rats to evaluate its antifungal activity against oral candidiasis in comparison with the marketed (Nystatin) oral suspension.

Fourier Transform Infrared (FTIR) Analysis

The infra-red spectra of Nystatin pure drug showed significant peaks at the given frequencies in cm^{-1}: 3300 to 3500, 2968.45, 1708.93, 1571.99, 1436.97, 1398.93, 1068.56. The frequency of 3300 to 3500 cm^{-1} indicates (NH, OH) stretching, 2936 cm^{-1} indicates (C-H) stretch (aliphatic, alkane), 1702 cm^{-1} indicates stretching vibration of carbonyl group (C=O),1577 and 1576 cm^{-1} indicates (COOH) carboxyl ion, 1597 cm^{-1} indicates (C=C) (aromatic stretch), 1490 and 1448 cm^{-1} indicates (CH2) (alkane), 1376 cm^{-1} indicates Symmetrical deformation of (CH3), 1065 cm^{-1} indicates Symmetrical stretching of (CH3), and 999 and 962 cm^{-1} indicates (=C-H) (aromatic, alkene).[92] The infrared spectra of the physical mixture of the components of SP3L1 in a (1:1) ratio of all ingredients (Drug: Span 80: SDC: CP349: Sugar: Corn Syrup: Beta-cyclodextrin: Acacia: Mannitol: Microcrystalline cellulose: Xanthan gum: orange oil flavor: Orange color) showed the similar characteristic peaks of the pure Nystatin powder at their respective wavelengths, that indicated the compatibility of Nystatin with the other used excipients, Figure 16.

Microbiological and Histopathological Findings of the Conducted in-vivo Study on Rats

The Quantitative Assay of the Candida Colony Formation Units (CFU) in the Rat's Oral Tissues Homogenates to Detect the Viable Count

The number of the colony-formation units of CA in the examined tenfold serial dilutions of the oral cavity homogenates of each group is presented in Table 8. The positive control group showed (3×10^6) ±22 CFU/mL, while the negative control group homogenates showed negative culture by the end of the experiment. The number of the colony formation

https://doi.org/10.2147/DDDT.S504768

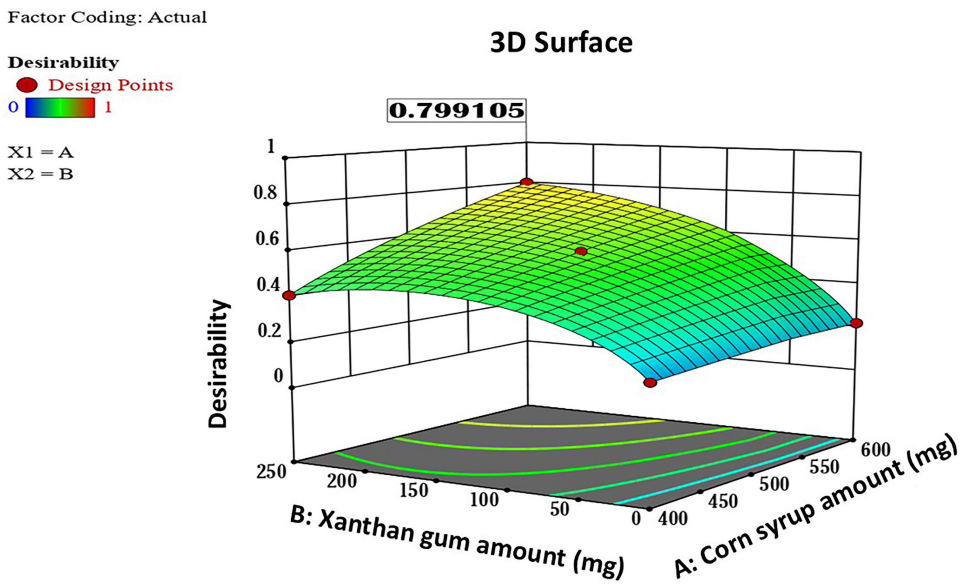

Figure 15 A 3D surface diagram showing the numerical desirability of the optimum Nystatin Spanlastical lozenges (SP3L1), where (A) is the corn syrup amount and (B) is the xanthan gum amount.

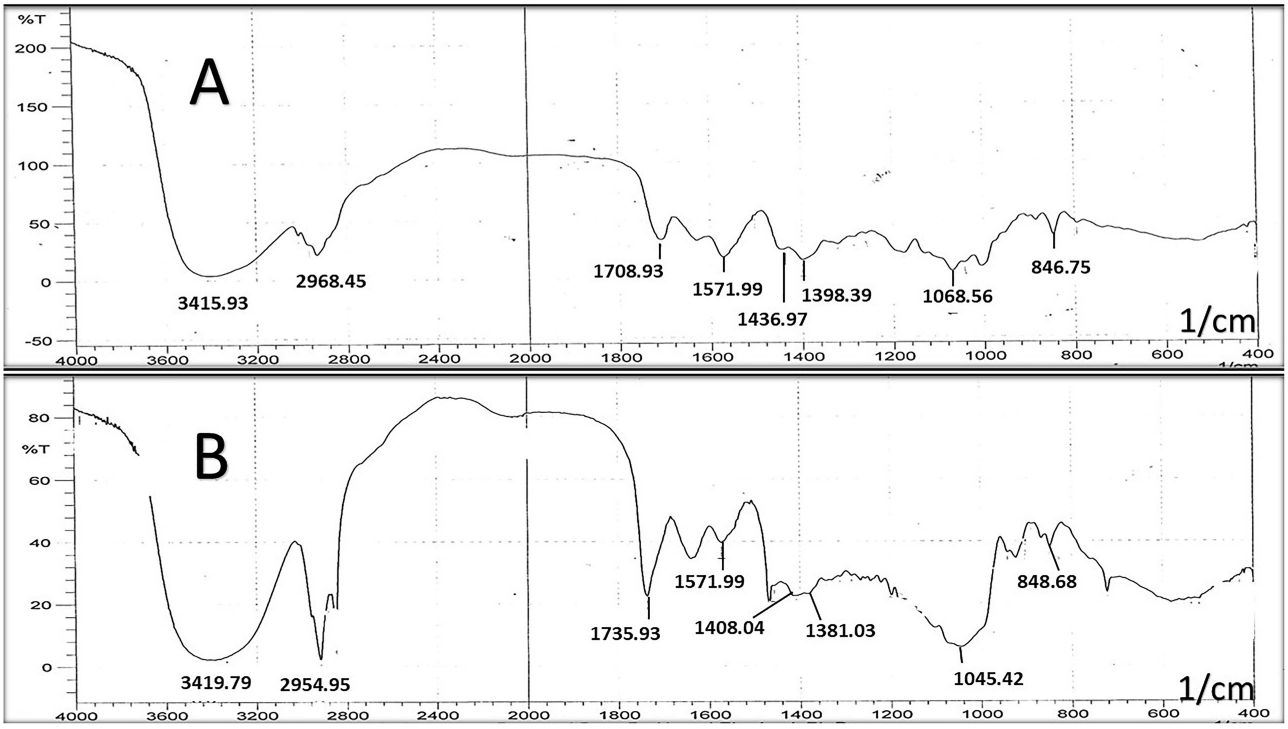

Figure 16 (**A**) FTIR Spectra of Nystatin pure powder, (**B**) FTIR Spectra of the physical mixture of (1:1) ratio of all ingredients of SP3L1 formulae (Drug: Span 80: SDC: Sugar: Corn Syrup: Beta-cyclodextrin: Acacia: Mannitol: Microcrystalline cellulose: Xanthan gum: Orange oil flavor: Orange Color FCF- E110).

units of the control groups was used as a reference. The CFU of the Group 1 subjects' homogenates (treated with the SP3L1) was (1×10^3) ±10 CFU/mL, while that of Gp2 subjects (treated with the market oral suspension (Nystatin)) was (2×10^6) ±35 CFU/mL. Upon statistically comparing the logarithm of the CFU of the four groups, it was found that there is a significant difference at $P \leq 0.05$ between SP3L1 and the other treatments (the market and control treatments). This considerable decrease in the Candida's viable count indicates that the study's optimum formula enhanced the Nystatin's microbiological activity against the tested Candida strain.

Table 8 The Logarithm of the Colony Formation Units (CFU) Obtained After the Quantitative Assay of the Oral Cavity Homogenates of the Rats of Each Group

Animal Group	Subjects Status Before Treatment	Treatment Administrated	CFU/mL	Logarithm of CFU/mL
Gp1	Infected	Optimum formula Sp3L1	($1x10^5$)	5
GP2	Infected	Market oral suspension (Nystatin)	($2x10^6$)	6.301
GP3 (Positive control)	Infected	Saline/agar solution	($3X10^6$)	6.477
GP4 (Negative control)	Normal	Saline/agar solution	Nil	Nil

The Morphological and Histopathological Findings

The morphology of the tongues of the control groups was used as a reference. The negative control group tongues were utterly normal, while the positive control group tongues showed inflamed white batches Figure 17 (A1, B1, A2, and B2). It was found that the tongues of rats treated with the optimum Nystatin Spanlastical lozenge SP3L1 had no signs of infection or inflammation; in contrast, those treated with the market formula (Nystatin) showed some redness and textural inflammation signs, Figure 17 (A3, B3, A4, and B4). Figures 18 and 19 show the histological photomicrography of the tissues of the oral cavity (stained with Hematoxylin and Eosin stain) of the subjects treated with the optimum prepared Nystatin Spanlastical oral lozenge SP3L1 and those treated with (Nystatin) marketed oral suspension, respectively. It was found that the examined tissues of the rat subjects treated with SP3L1 (GP1) showed no signs of inflammation lesions or infection signs; they also showed no presence of any Candida cells upon being stained with the PAS stain. In contrast, the group treated with the marketed oral Nystatin suspension (GP2) showed some congestions that reflect incomplete

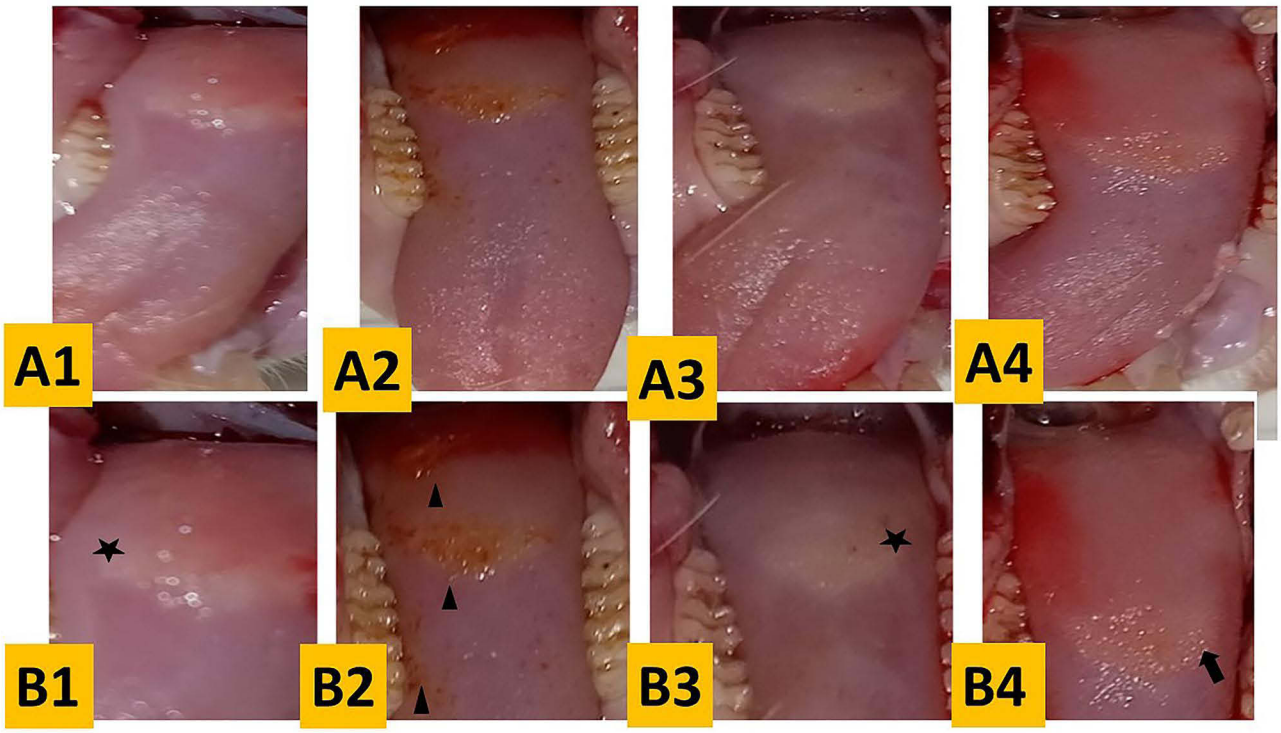

Figure 17 (**A**) Morphology of the rat subject's whole tongues that include the apex, the anterior portion of the lingual body, the protuberance, and the posterior portion of the lingual body; (A1) Negative control group (4th group), (A2) Positive control group (3rd group), (A3) group treated with the optimum prepared Nystatin Spanlastical candy lozenge SP3L1 (1st group), (A4) group (treated with the (Nystatin) marketed oral suspension (2nd group); (**B**) Intermolar eminence and fungiform papillae regions; (B1) 4th group with normal morphology (Star), (B2) 3rd group with whitish regions and papillary atrophy (arrowhead), (B3) 1st group with a normal morphology (Star), (B4) 4th group with inflammation signs (arrow).

https://doi.org/10.2147/DDDT.S504768

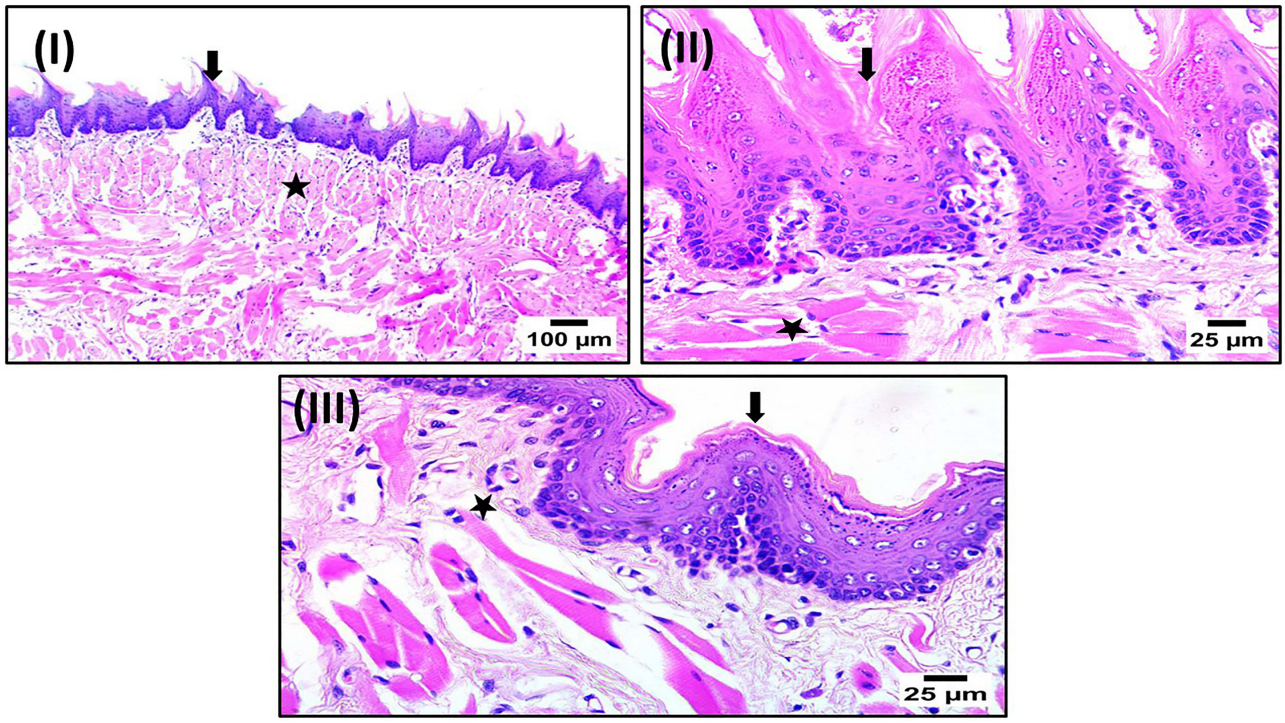

Figure 18 Light microscope photomicrograph of the tongue and oral cavity of the rats of the first group (treated with the optimum prepared Nystatin Spanlastical candy lozenge SP3L1); (**I**) photomicrograph showing a normal histological structure of tongue including filiform papillae (arrow) and submucosa (star) (Hematoxylin and Eosin stain) with a magnification power of 100X, (**II**) photomicrograph showing a normal histological structure of tongue including filiform papillae (arrow) and submucosa (star) (Hematoxylin and Eosin stain) with a magnification power of 400X, (**III**) photomicrograph showing normal histological structure of oral epithelium (arrow) and lamina propria (star) (Hematoxylin and Eosin stain) with magnification power of 400X.

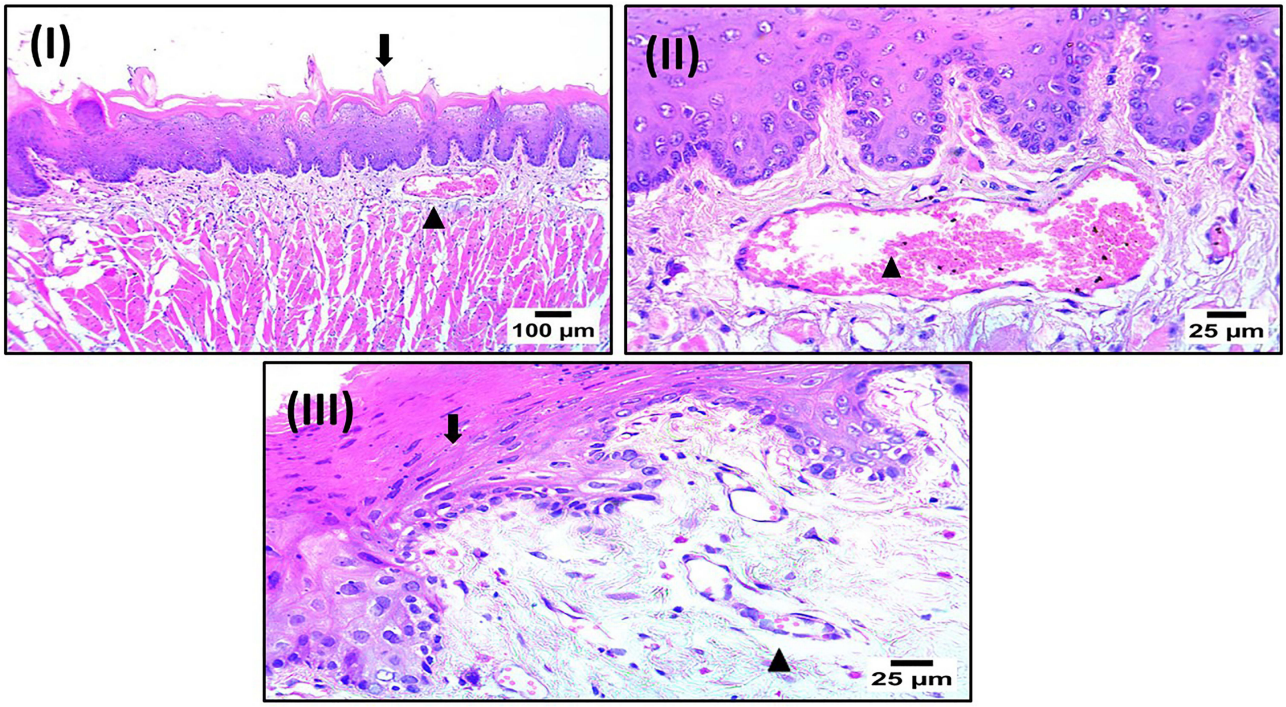

Figure 19 Light microscope photomicrograph of the tongue and oral cavity of the rats of the second group (treated with the (Nystatin) marketed oral suspension); (**I**) photomicrograph showing normal lingual papillae (arrow) with congestion of submucosal blood vessels (arrowhead) (Hematoxylin and Eosin stain) with a magnification power of 100X, (**II**) photomicrograph showing congestion of submucosal blood vessels (arrowhead) (Hematoxylin and Eosin stain) with a magnification power of 400X, (**III**) photomicrograph showing a normal histological structure of oral epithelium (arrow) with mild congestion of submucosal blood vessels (arrowhead) (Hematoxylin and Eosin stain) with magnification power of 400X.

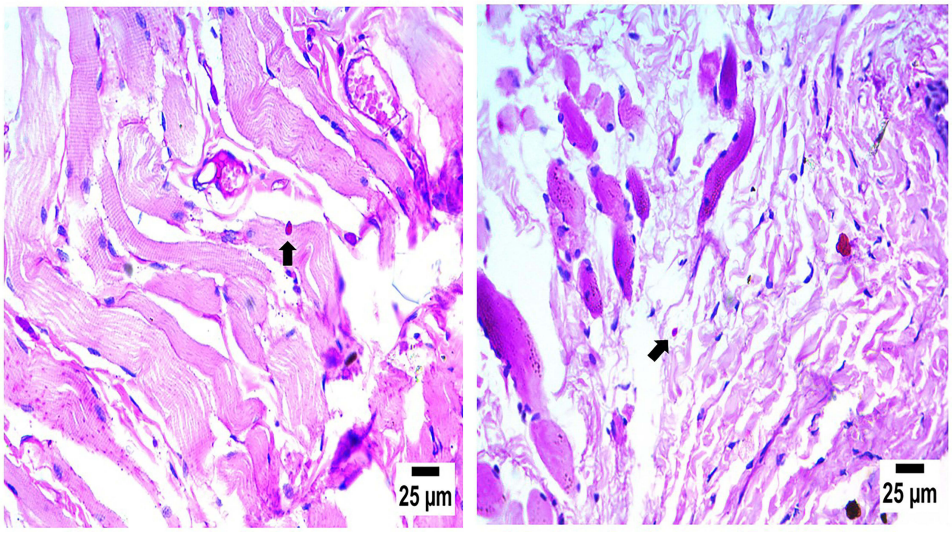

Figure 20 Light microscope photomicrograph showing a single cell of candida sp. (arrow) in the submucosa of the second group (treated with the (Nystatin) marketed oral suspension) (PAS stain) with a magnification power of 400X.

healing; they also showed a presence of Candida cells upon being stained with the PAS stain, as illustrated in Figure 20. These results can also indicate the enhanced antifungal activity of the SP3L1 preparation over the marketed formula.

Conclusion

Oral candidiasis is common in children and the elderly, especially those who were treated for an extended period with antibiotics or chemotherapy. The current study presents an optimized Nystatin mucoadhesive Spanlastical solid candy lozenge for the local treatment of oral candidiasis. The candy formula provides an attractive, sweet mucoadhesive presentation of the nanosized Nystatin (Spanlastics) to the patient's oral cavity. The in vitro characterization, in addition to the in-vivo study on rats, revealed that the optimum formula (SP3L1) was very effective as it showed a significant reduction in the count of the colony formation units in the oral cavity of the examined rats. The morphological and histopathological findings also confirmed the enhanced activity of SP3L1, as rats treated with it showed very normal oral tissues by the end of the study period compared to those treated with the market oral formula (Nystatin). Therefore, this approach that merges nanotechnology with mucoadhesive lozenging can be promising for treating local oral diseases such as candidiasis with an enhanced taste, residence, and activity.

Future clinical studies should be conducted to assess and validate the safety and efficacy of Nystatin spanlastical lozenges on patients upon long-term use. Also, investigations of the patient-reported outcomes, such as symptom relief and compliance enhancement, should be monitored.

Ethical Approval Statement

The study was approved by the research ethics committee at the College of Pharmaceutical Sciences and Drug Manufacturing, Misr University for Science and Technology, Giza, Egypt (Code: IP06).

Acknowledgment

The authors are thankful to the Assistant Lecturer Dr. Wesam El-Sayed (Microbiology Department, College of Pharmaceutical Sciences and Drug Manufacturing, Misr University for Science and Technology, Giza, Egypt) for her valuable contribution to the microbiological investigations. The authors are also grateful to Dr. Khaled El-Refai, Ph.D. of pharmaceutics (Egyptian Drug Authority, Cairo, Egypt), and Prof. Dr. Sabah M. Moltazem (Analytical Chemistry, Bisha University, KSA) for their outstanding support throughout the work period.

Funding

This research received no external funding.

Disclosure

The authors declare no conflicts of interest.

References

1. Tewabe A, Abate A, Tamrie M, Seyfu A, Siraj EA. Targeted drug delivery: from magic bullet to nanomedicine—principles, challenges, and future perspectives. *J Multidiscip Healthc*. 2021;14:1711–1724. doi:10.2147/JMDH.S313968
2. Srivastava N, Aslam S. Recent advancements and patents on buccal drug delivery systems: a comprehensive review. *Recent Pat Nanotechnol*. 2022;16(4):308–325. doi:10.2174/1872210515666210609145144
3. Kulkarni MP, Sharma A, Tanwar S, et al. Pharmaceutical lozenges: recent trends and developments with an update on research and patents. *Recent Adv Drug Deliv Formul*. 2022;16(1):45–54. doi:10.2174/2667387816666211231103759
4. Hemilä H, Haukka J, Alho M, Vahtera J, Kivimäki M. Zinc acetate lozenges for the treatment of the common cold: a randomised controlled trial. *BMJ Open*. 2020;10(1):e031662. doi:10.1136/bmjopen-2019-031662
5. Ansari MD, Saifi Z, Pandit J, et al. Spanlastics: a novel nanovesicular carrier—its potential application and emerging trends in therapeutic delivery. *AAPS PharmSciTech*. 2022;23(4):112. doi:10.1208/s12249-022-02217-9
6. Elhabak M, Ibrahim S, Abouelatta SM. Topical delivery of L-ascorbic acid spanlastics for stability enhancement and treatment of UVB-induced damaged skin. *Drug Deliv*. 2021;28(1):445–453. doi:10.1080/10717544.2021.1886377
7. Lyu X, Zhao C, Yan ZM, Hua H. Efficacy of nystatin for the treatment of oral candidiasis: a systematic review and meta-analysis. *Drug Des Dev Ther*. 2016;10:1161–1171. doi:10.2147/DDDT.S100795
8. Kaur IP, Kakkar S. Topical delivery of antifungal agents. *Expert Opin Drug Deliv*. 2010;7(11):1303–1327. doi:10.1517/17425247.2010.525230
9. Zaki RM, Ibrahim MA, Alshora DH, Ela AESA E. Formulation and evaluation of transdermal gel containing tacrolimus-loaded spanlastics: in vitro, ex vivo, and in vivo studies. *Polymers*. 2022;14(8):1528. doi:10.3390/polym14081528
10. Saini H, Rapolu Y, Razdan K, Nirmala, Sinha VR. Spanlastics: a novel elastic drug delivery system with potential applications via multifarious routes of administration. *J Drug Target*. 2023;31(10):999–1012. doi:10.1080/1061186X.2023.2274805
11. Yadav NK, Nanda S, Sharma G, Katare OP. Systematically optimised ketoprofen-loaded novel proniosomal formulation for periodontitis: in vitro characterization and in vivo pharmacodynamic evaluation. *AAPS PharmSciTech*. 2017;18(5):1863–1880. doi:10.1208/s12249-016-0665-1
12. Jiang J, Ma T, Zhang L, Cheng X, Wang C. The transdermal performance, pharmacokinetics, and anti-inflammatory pharmacodynamics evaluation of harmine-loaded ethosomes. *Drug Dev Ind Pharm*. 2020;46(1):101–108. doi:10.1080/03639045.2019.1706549
13. Abdelbary AA, Abd-Elsalam WH, Al-Mahallawi AM. Fabrication of novel ultradeformable bilosomes for enhanced ocular delivery of terconazole: in vitro characterization, ex vivo permeation, and in vivo safety assessment. *Int J Pharm*. 2016;513(1–2):688–696. doi:10.1016/j.ijpharm.2016.10.006
14. Mosallam S, Sheta NM, Elshafeey AH, Abdelbary AA. Fabrication of highly deformable bilosomes for enhancing the topical delivery of terconazole: in vitro characterization, microbiological evaluation, and in vivo skin deposition study. *AAPS PharmSciTech*. 2021;22(2):74. doi:10.1208/s12249-021-01924-z
15. Daneshmand S, Golmohammadzadeh S, Jaafari MR, et al. Encapsulation challenges: the substantial issue in solid lipid nanoparticles characterization. *J Cell Biochem*. 2018;119(6):4251–4264. doi:10.1002/jcb.26617
16. Koirala S, Nepal P, Ghimire G, et al. Formulation and evaluation of mucoadhesive buccal tablets of aceclofenac. *Heliyon*. 2021;7(3):e06439. doi:10.1016/j.heliyon.2021.e06439
17. El-Hadidy GN A pharmaceutical study on topical antifungal drug. MSc thesis, Cairo Univ, Fac Pharm, Cairo, Egypt; 2010.
18. Al-Mahallawi AM, Khowessah OM, Shoukri RA. Nano-transfersomal ciprofloxacin-loaded vesicles for non-invasive trans-tympanic ototopical delivery: in vitro optimization, ex vivo permeation studies, and in vivo assessment. *Int J Pharm*. 2014;472(1–2):304–314. doi:10.1016/j.ijpharm.2014.06.041
19. Patel P, Madan P, Lin S. Formulation and evaluation of time-controlled triple-concentric mefenamic acid tablets for rheumatoid arthritis. *Pharm Dev Technol*. 2014;19(3):355–362. doi:10.3109/10837450.2013.788514
20. Lupo N, Jalil A, Nazir I, Gust R, Bernkop-Schnürch A. In vitro evaluation of intravesical mucoadhesive self-emulsifying drug delivery systems. *Int J Pharm*. 2019;564:180–187. doi:10.1016/j.ijpharm.2019.04.035
21. Shen J, Burgess DJ. In vitro dissolution testing strategies for nanoparticulate drug delivery systems: recent developments and challenges. *Drug Deliv Transl Res*. 2013;3(5):409–415. doi:10.1007/s13346-013-0129-z
22. Susan D. A review of in vitro drug release test methods for nano-sized dosage forms: review article. *Adv Pharm*. 2014;304757:12.
23. Abbasnezhad N, Zirak N, Champmartin S, Shirinbayan M, Bakir F. An overview of in vitro drug release methods for drug-eluting stents. *Polymers*. 2022;14(13):2751. doi:10.3390/polym14132751
24. Tietz K, Klein S. In vitro methods for evaluating drug release of vaginal ring formulations—a critical review. *Pharmaceutics*. 2019;11(10):538. doi:10.3390/pharmaceutics11100538
25. Scognamiglio I, De Stefano D, Campani V, et al. Nanocarriers for topical administration of resveratrol: a comparative study. *Int J Pharm*. 2013;440(2):179–187. doi:10.1016/j.ijpharm.2012.08.009
26. Danaei M, Dehghankhold M, Ataei S, et al. Impact of particle size and polydispersity index on the clinical applications of lipidic nanocarrier systems. *Pharmaceutics*. 2018;10(2):57. doi:10.3390/pharmaceutics10020057
27. Tzeyung AS, Md S, Bhattamisra SK, et al. Fabrication, optimisation, and evaluation of rotigotine-loaded chitosan nanoparticles for nose-to-brain delivery. *Pharmaceutics*. 2019;11(1):26. doi:10.3390/pharmaceutics11010026
28. Bate S, Karp NA. A common control group—optimising the experiment design to maximise sensitivity. *PLoS One*. 2014;9(12):e114872. doi:10.1371/journal.pone.0114872

29. Smith MM, Clarke EC, Little CB. Considerations for the design and execution of protocols for animal research and treatment to improve reproducibility and standardisation: "DEPART well-prepared and ARRIVE safely". *Osteoarthritis Cartilage*. 2017;25(3):354–363. doi:10.1016/j.joca.2016.10.016
30. Hossain ML, Lim LY, Hammer K, Hettiarachchi D, Locher C. A review of commonly used methodologies for assessing the antibacterial activity of honey and honey products. *Antibiotics*. 2022;11(7):975. doi:10.3390/antibiotics11070975
31. Güler Ş, Torul D, Kurt-Bayrakdar S, Tayyarcan EK, Çamsarı Ç, Boyacı İH. Evaluation of antibacterial efficacy of Lawsonia inermis Linn (henna) on periodontal pathogens using agar well diffusion and broth microdilution methods: an in-vitro study. *BioMedicine*. 2023;13(3):25. doi:10.37796/2211-8039.1411
32. Donato R, Sacco C, Pini G, Bilia AR. Antifungal activity of different essential oils against Malassezia pathogenic species. *J Ethnopharmacol*. 2020;249:112376. doi:10.1016/j.jep.2019.112376
33. Pelourde C, Bationo R, Boileau MJ, Colat-Parros J, Jordana F. Monomer release from orthodontic retentions: an in vitro study. *Am J Orthod Dentofacial Orthop*. 2018;153(2):248–254. doi:10.1016/j.ajodo.2017.06.021
34. Chanda R, Nallaguntla L. Formulation and evaluation of medicated lozenges for sore throat. *Asian J Pharm Clin Res*. 2020;13(10):62–67. doi:10.22159/ajpcr.2020.v13i10.38660
35. Tietz K, Gutknecht SI, Klein S. Bioequivalence of locally acting lozenges: evaluation of critical in vivo parameters and first steps towards a bio-predictive in-vitro test method. *Eur J Pharm Biopharm*. 2018;123:71–83. doi:10.1016/j.ejpb.2017.11.011
36. Ozel B, Kuzu S, Marangoz MA, Dogdu S, Morris RH, Oztop MH. Hard candy production and quality parameters: a review. *Open Res Eur*. 2024;4(60):60. doi:10.12688/openreseurope.16792.1
37. Hayashi H, Kobayashi R, Suzuki A, et al. Preparation and clinical evaluation of a novel lozenge containing polaprezinc, a zinc-L-carnosine, for prevention of oral mucositis in patients with hematological cancer who received high-dose chemotherapy. *Med Oncol*. 2016;33(8):91. doi:10.1007/s12032-016-0795-z
38. Sripetch S, Prajapati M, Loftsson T. Cyclodextrins and drug membrane permeation: thermodynamic considerations. *J Pharm Sci*. 2002;111(9):2571–2580. doi:10.1016/j.xphs.2022.04.015
39. Appleton SL, Navarro-Orcajada S, Martínez-Navarro FJ, et al. Cyclodextrins as anti-inflammatory agents: basis, drugs, and perspectives. *Biomolecules*. 2021;11(9):1384. doi:10.3390/biom11091384
40. Zimmer Ł, Kasperek R, Poleszak E. Zastosowanie β-cyklodekstryn w formulacji tabletek ODT zawierających ibuprofen [Application of β-cyclodextrin in the formulation of ODT tablets containing ibuprofen]. *Polimery Med*. 2014;44(4):231–235. doi:10.17219/pim/30770
41. Naseem S, Gupta D, Koshyari H. Evaluation of the efficacy of turmeric-based lozenges for the prevention of postoperative sore throat in surgeries done under laryngeal mask airway insertion. *Anaesth Essent Res*. 2022;16(2):213–218. doi:10.4103/aer.aer_56_22
42. Kurćubić I, Vajić UJ, Cvijić S, et al. Mucoadhesive buccal tablets with propranolol hydrochloride: formulation development and in vivo performances in experimental essential hypertension. *Int J Pharm*. 2021;610:121266. doi:10.1016/j.ijpharm.2021.121266
43. Javed QUA, Syed MA, Arshad R, et al. Evaluation and optimisation of prolonged release mucoadhesive tablets of dexamethasone for wound healing: in vitro-in vivo profiling in healthy volunteers. *Pharmaceutics*. 2022;14(4):807. doi:10.3390/pharmaceutics14040807
44. Musial W, Mielck JB. The application of modified flow-through cell apparatus for the assessment of chlorhexidine dihydrochloride release from lozenges containing sorbitol. *AAPS PharmSciTech*. 2009;10(3):1048–1057. doi:10.1208/s12249-009-9298-y
45. Nair AB, Shah J, Jacob S, et al. Development of mucoadhesive buccal film for rizatriptan: in vitro and in vivo evaluation. *Pharmaceutics*. 2021;13(5):728. doi:10.3390/pharmaceutics13050728
46. Çelik B. Risperidone mucoadhesive buccal tablets: formulation design, optimisation and evaluation. *Drug Des Devel Ther*. 2017;11:3355–3365. doi:10.2147/DDDT.S150774
47. Kottke D, Majid H, Breitkreutz J, Burckhardt BB. Development and evaluation of mucoadhesive buccal dosage forms of lidocaine hydrochloride by ex-vivo permeation studies. *Int J Pharm*. 2020;581:119293. doi:10.1016/j.ijpharm.2020.119293
48. Abdelmonem R, Hamed RR, Abdelhalim SA, ElMiligi MF, El-Nabarawi MA. Formulation and characterization of cinnarizine targeted aural transfersomal gel for vertigo treatment: a pharmacokinetic study on rabbits. *Int J Nanomedicine*. 2020;15:6211–6223. doi:10.2147/IJN.S258764
49. Gomaa E, El Deeb S, Ibrahim AE, Faisal MM. Bimodal release two-in-one clonazepam matrix lozenge tablets for managing anxiety-related disorders: formulation, optimization and in vivo evaluation. *Scientia Pharmaceutica*. 2022;90(3):43. doi:10.3390/scipharm90030043
50. Wiegand S, Berner R, Schneider A, Lundershausen E, Dietz A. Otitis externa: investigation and evidence-based treatment. *Dtsch Arztebl Int*. 2019;116(13):224–234. doi:10.3238/arztebl.2019.0224
51. Althobaiti YS. Role of venlafaxine in relapse to methamphetamine seeking. Potential treatment option for drug dependence. *Saudi Med J*. 2019;40(4):339–346. doi:10.15537/smj.2019.4.23718
52. Radithia D, Tanjungsari R, Ernawati DS, Parmadiati AE. The effectiveness of essential oil from Citrus limon peel on Candida albicans biofilm formation: an experimental in vivo study. *J Taibah Univ Med Sci*. 2023;18(1):190–195. doi:10.1016/j.jtumed.2022.07.011
53. El-Newary SA, Abd Elkarim AS, Abdelwahed NA, Omer EA, Elgamal AM, ElSayed WM. Chenopodium murale juice shows anti-fungal efficacy in experimental oral candidiasis in immunosuppressed rats in relation to its chemical profile. *Molecules*. 2023;28(11):4304. doi:10.3390/molecules28114304
54. Mutuku A, Mwamburi L, Keter L, et al. Evaluation of the antimicrobial activity and safety of Rhus vulgaris (Anacardiaceae) extracts. *BMC Complement Med Ther*. 2020;20:1–2. doi:10.1186/s12906-020-03063-7
55. Pérez-Sayáns M, Beiro-Fuentes R, Otero-Rey EM, et al. Efficacy of different formulations of nystatin in an experimental model of oral candidiasis in sialoadenectomized rats. *J Dent Sci*. 2021;16(1):123–130. doi:10.1016/j.jds.2020.05.031
56. Rex TS, Boyd K, Apple T, Bricker-Anthony C, Vail K, Wallace J. Effects of repeated anesthesia containing urethane on tumor formation and health scores in male C57BL/6J mice. *J Am Assoc Lab Anim Sci*. 2016;55(3):295–299.
57. Schulten L, Spillner J, Kanzler S, Teubner A, Jockenhoevel S, Apel C. A polyurethane-based surgical adhesive for sealing blood vessel anastomoses—A feasibility study in pigs. *J Biomed Mater Res B Appl Biomater*. 2022;110(8):1922–1931. doi:10.1002/jbm.b.35049
58. Goździewska-Harłajczuk K, Klećkowska-Nawrot J, Barszcz K, et al. Biological aspects of the tongue morphology of wild-captive WWCPS rats: a histological, histochemical and ultrastructural study. *Anat Sci Int*. 2018;93:514–532. doi:10.1007/s12565-018-0445-y

59. Thomas P, Sekhar AC, Upreti R, Mujawar MM, Pasha SS. Optimization of single plate-serial dilution spotting (SP-SDS) with sample anchoring as an assured method for bacterial and yeast cfu enumeration and single colony isolation from diverse samples. *Biotechnol Rep*. 2015;8:45–55. doi:10.1016/j.btre.2015.08.003
60. Okada M, Hisajima T, Ishibashi H, Miyasaka T, Abe S, Satoh T. Pathological analysis of the Candida albicans-infected tongue tissues of a murine oral candidiasis model in the early infection stage. *Arch Oral Biol*. 2013;58(4):444–450. doi:10.1016/j.archoralbio.2012.09.014
61. de Haan K, Zhang Y, Zuckerman JE, et al. Deep learning-based transformation of H&E stained tissues into special stains. *Nat Commun*. 2021;12(1):1–3. doi:10.1038/s41467-021-25221-2
62. Mazyed EA, Helal DA, Elkhoudary MM, Abd Elhameed AG, Yasser M. Formulation and optimization of nanospanlastics for improving the bioavailability of green tea epigallocatechin gallate. *Pharmaceuticals*. 2021;14(1):68. doi:10.3390/ph14010068
63. Naik S, Mullick P, Mutalik SP, et al. Full factorial design for development and validation of a stability-indicating RP-HPLC method for the estimation of timolol maleate in surfactant-based elastic Nano-vesicular systems. *J Chromatogr Sci*. 2022;60(6):584–594. doi:10.1093/chromsci/bmab101
64. Ly HH, Daniel S, Soriano SKV, Kis Z, Blakney AK. Optimisation of lipid nanoparticles for saRNA expression and cellular activation using a design-of-experiment approach. *mol Pharm*. 2022;19(6):1892–1905. doi:10.1021/acs.molpharmaceut.2c00032
65. Bnyan R, Khan I, Ehtezazi T, et al. Surfactant effects on lipid-based vesicles properties. *J Pharm Sci*. 2018;107(5):1237–1246. doi:10.1016/j.xphs.2018.01.005
66. Badawi N, El-Say K, Attia D, El-Nabarawi M, Elmazar M, Teaima M. Development of pomegranate extract-loaded solid lipid nanoparticles: quality by design approach to screen the variables affecting the quality attributes and characterization. *ACS Omega*. 2020;5(34):21712–21721. doi:10.1021/acsomega.0c02618
67. Hady MA, Darwish AB, Abdel-Aziz MS, Sayed OM. Design of transfersomal nanocarriers of nystatin for combating vulvovaginal candidiasis: a different perspective. *Colloids and Surfaces B*. 2022;211:112304. doi:10.1016/j.colsurfb.2021.112304
68. Abdallah MH, Shahien MM, Alshammari A, et al. The exploitation of sodium deoxycholate-stabilized nano-vesicular gel for ameliorating the antipsychotic efficiency of sulpiride. *Gels*. 2024;10(4):239. doi:10.3390/gels10040239
69. Abdelbari MA, El-Mancy SS, Elshafeey AH, Abdelbary AA. Implementing spanlastics for improving the ocular delivery of clotrimazole: in vitro characterization, ex vivo permeability, microbiological assessment and in vivo safety study. *Int J Nanomedicine*. 2021;10:6249–6261. doi:10.2147/IJN.S319348
70. Badria F, Mazyed E. Formulation of nanoSpanlastics as a promising approach for improving the topical delivery of a natural leukotriene inhibitor (3-acetyl-11-keto-β-boswellic acid): statistical optimization, in vitro characterization, and ex vivo permeation study. *Drug Des Devel Ther*. 2020;15:3697–3721. doi:10.2147/DDDT.S265167
71. Elsherif NI, Shamma RN, Abdelbary G. Terbinafine hydrochloride trans-ungual delivery via nanovesicular systems: in vitro characterization and ex vivo evaluation. *AAPS PharmSciTech*. 2017;18(2):551–562. doi:10.1208/s12249-016-0528-9
72. Al-Mahallawi AM, Khowessah OM, Shoukri RA. Enhanced non-invasive trans-tympanic delivery of ciprofloxacin through encapsulation into nano-Spanlastic vesicles: fabrication, in-vitro characterization, and comparative ex-vivo permeation studies. *Int J Pharm*. 2017;522(1–2):157–164. doi:10.1016/j.ijpharm.2017.03.005
73. ElMeshad AN, Mohsen AM. Enhanced corneal permeation and antimycotic activity of itraconazole against Candida albicans via a novel nanosystem vesicle. *Drug Deliv*. 2016;23(7):2115–2123. doi:10.3109/10717544.2014.942811
74. Diksha KP, Verma N. To investigate the effect of span 60 and span 80 polymer on release rate of simvastatin noisome in comparison with pure simvastatin. *IJPSR*. 2021;12(7):3799–3804.
75. El-Say KM, Abd-Allah FI, Lila AE, Hassan Ael S, Kassem AE. Diacerein niosomal gel for topical delivery: development, in vitro and in vivo assessment. *J Liposome Res*. 2016;26(1):57–68. doi:10.3109/08982104.2015.1029495
76. Raval N, Maheshwari R, Kalyane D, Youngren-Ortiz SR, Chougule MB, Tekade RK. Importance of physicochemical characterisation of nanoparticles in pharmaceutical product development. In: *Basic Fundamentals of Drug Delivery*. 2019:369–400.
77. Fadaei MS, Fadaei MR, Kheirieh AE, et al. Niosome as a promising tool for increasing the effectiveness of anti-inflammatory compounds. *EXCLI J*. 2024;23:212. doi:10.17179/excli2023-6868
78. Smith MC, Crist RM, Clogston JD, McNeil SE. Zeta potential: a case study of cationic, anionic, and neutral liposomes. *Anal Bioanal Chem*. 2017;409(24):5779–5787. doi:10.1007/s00216-017-0527-z
79. Sadat Hosseini M, Kamali B, Nabid MR. Multilayered mucoadhesive hydrogel films based on Ocimum basilicum seed mucilage/thiolated alginate/dopamine-modified hyaluronic acid and PDA coating for sublingual administration of Nystatin. *Int J Biol Macromol*. 2022;203:93–104. doi:10.1016/j.ijbiomac.2022.01.031
80. Shukr MH, Ismail S, El-Hossary GG, El-Shazly AH. Spanlastics nanovesicular ocular insert as a novel ocular delivery of travoprost: optimisation using box-behnken design and in vivo evaluation. *J Liposome Res*. 2022;32(4):354–364. doi:10.1080/08982104.2022.2025828
81. Safhi AY, Naveen NR, Rolla KJ, et al. Enhancement of antifungal activity and transdermal delivery of 5-flucytosine via tailored Spanlastic nanovesicles: statistical optimization, in-vitro characterization, and in-vivo biodistribution study. *Front Pharmacol*. 2023;14:1321517. doi:10.3389/fphar.2023.1321517
82. Moon KN, Baek SK, Kim W, et al. Prenatal developmental toxicity study of 2, 4-dichlorobenzyl alcohol in rats. *Regul Toxicol Pharmacol*. 2022;132:105168. doi:10.1016/j.yrtph.2022.105168
83. Jadav M, Pooja D, Adams DJ, Kulhari H. Advances in xanthan gum-based systems for the delivery of therapeutic agents. *Pharmaceutics*. 2023;15(2):402. doi:10.3390/pharmaceutics15020402
84. Majekodunmi SO. A review on lozenges. *Am J Med Med Sci*. 2015;5(2):99–104.
85. Choursiya S, Andheriya D. Review on lozenges. *J Drug Deliv Ther*. 2018;8(6–A):124–128.
86. Rathod M, Poharkar S, Pandhre Y, Muneshwar M, Sul S. Medicated lozenges as an easy-to-use dosage form. *World J Pharm Res*. 2018;7(16):305–322.
87. Zhao H, Yu Y, Ni N, et al. A new parameter for characterization of tablet friability based on a systematical study of five excipients. *Int J Pharm*. 2022;61:121339. doi:10.1016/j.ijpharm.2021.121339

88. Vashchenko OV, Brodskii RY, Davydova IO, Vashchenko PV, Ivaniuk OI, Ruban OA. Biopharmaceutical studies of a novel sedative sublingual lozenge based on glycine and tryptophan: a rationale for mucoadhesive agent selection. *Eur J Pharm Biopharm*. 2024;203:114469. doi:10.1016/j.ejpb.2024.114469
89. Terescenco D, Hadj Benali L, Canivet F, et al. Bio-sourced polymers in cosmetic emulsions: a hidden potential of the alginates as thickeners and gelling agents. *Int J Cosmet Sci*. 2021;43(5):573–587. doi:10.1111/ics.12732
90. Yamsani MR, Kumar YS, Sandeep P, Nomula N, Avinash M. Formulation and evaluation of lidocaine lozenges. *Int J Innov Res Sci Eng Technol*. 2015;4(11):11640–11647.
91. Chandrawanshi MJ, Sakhare RS, Nagoba SN, Bhalekar RV. A review on medicated lozenges. *World J Pharm Res*. 2019;8(2):396–412.
92. El-Batal AI, Nada HG, El-Behery RR, Gobara M, El-Sayyad GS. Nystatin-mediated bismuth oxide nano-drug synthesis using gamma rays for increasing the antimicrobial and antibiofilm activities against some pathogenic bacteria and Candida species. *RSC Adv*. 2020;10(16):9274–9289. doi:10.1039/C9RA10765G